Assessment of Heavy Metal Fluxes and Radiation Exposure due to NORM in the Extraction and Processing of Coltan Ores in Selected Areas of Rwanda

By

NTIHABOSE Léon
B.Sc. (Hons)

A thesis submitted in partial fulfillment of the requirements for the award of Master of Science (MSc) degree in Physics, University of Nairobi.
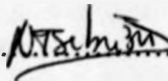
October, 2010

DECLARATION

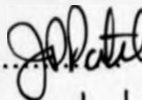This thesis is my own work and has not been examined or submitted for examination in any other university.

NTIHABOSE Léon

Signature.~~N.Txhu?u~~....
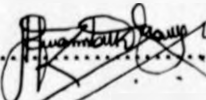
Date... 26.11.01.2010...

This thesis has been submitted for examination with the approval of my University supervisors:

1) Prof. J.P. Patel
Department of Physics
University of Nairobi

Signature.......~~JMPatil~~

Date................26.10.10

2) Dr. H.K. Angeyo
Department of Physics
University of Nairobi

Signature.~~...~~

Date................26-10-2010

3) Mr. D.M. Maina
Institute of Nuclear Science & Technology
University of Nairobi

Signature.~~...~~

Date. 27/10/2010....

DEDICATION

To my mother, late father, brothers, sisters and friends.

ACKNOWLEDGEMENTS

ABSTRACT

The present study quantifies heavy metal fluxes and radiation exposure due to Naturally Occurring Radioactive Materials (NORM) in the extraction and processing of the Columbite-Tantalite (Coltan) mineral in Muhanga, Ruli and Ngoma areas of Rwanda. Heavy metal in samples of Coltan ore, mine sediments and soil from the three areas were analyzed using the Energy Dispersive X-Ray Fluorescence (EDXRF) spectrometry. Activity concentrations of primordial radionuclides ^{40}K, ^{238}U and ^{232}Th in samples of Coltan, sediments and soil were determined by Hyper Pure Germanium (HPGe)-based gamma-ray spectrometry. Multivariate chemometrics techniques, Principal Component Analysis (PCA) and Hierarchical Cluster Analysis (HCA) were used to explore the salient relationships among measured data (heavy metals, radionuclides). The heavy metals were categorized into three classes which may be interpreted as, elements normally associated with coltan; radioactive minerals; and heavy metal toxic elements. Multivariate chemometrics techniques enabled to classify the samples into three coltan types namely; processed coltan, extracted (or unprocessed) coltan, mine sediments and control soil samples. Processed coltan is purified coltan which is obtained after separating soil and coltan by using water. Extracted coltan is the raw ore taken immediately from soil; it is a mixture of coltan and soil. Sediments are the wastes produced after removing coltan. Control soil sample is the soil which was taken from an area within the vicinity but outside the mining site. Coltan ore were also classified according to their origin using principal component analysis (PCA).

The result of elemental analysis showed that the most abundant elements were Tantalum (Ta), Niobium (Nb) and Tin (Sn). These elements are normally associated with Coltan. The highest

v

concentration of Ta (30.6 %), Nb (25.7 %) and Sn (16.4%) were observed in processed Coltan. In some sediment samples Ta (35.6-63.3 $\mu g \ g^{-1}$) and Nb (35.4-83.8 $\mu g \ g^{-1}$) were also reported but at lower level. Heavy toxic elements such as lead (Pb), manganese (Mn) and zinc (Zn) were also observed in all samples with manganese having the highest concentration (35,155-65,200) $\mu g \ g^{-1}$ and lead having the lowest concentration (548-1655) $\mu g \ g^{-1}$. Radioactive elements (U, Th, K) were detected in all samples with the highest concentration found in processed Coltan (115-569) $\mu g \ g^{-1}$, (281-797) $\mu g \ g^{-1}$ and (15,870-37,900) $\mu g \ g^{-1}$ respectively.

The average activity concentration of ^{238}U (513 Bq kg^{-1}) and ^{232}Th (57 Bq kg^{-1}) in all sample exceed the world wide average of ^{238}U (35Bq kg^{-1}) and ^{232}Th (30 Bq kg^{-1}), while the average ^{40}K (267 Bq kg^{-1}) activity was below the world wide average of 400 Bq kg^{-1}. Absorbed dose was obtained by measurement and models of calculation. In general the measured absorbed dose was found to be 2 times higher than the calculated absorbed dose. The measured absorbed dose varied 507.43-845.71 nGy h^{-1} (average: 665.5 nGy h^{-1}), whereas the calculated absorbed doses varied 63.52-779.07nGy h^{-1} (average: 286.19 nGy h^{-1}). These values are 5-11 times higher than the world wide average absorbed dose reported by UNSCEAR which is 55 nGy h^{-1}. This characterized the sampled areas of Rwanda as High Background Radiation Area (HBRA). Among the exposure pathways considered, inhalation of Coltan bearing dust resulted in the highest doses exposures from crushing and sieving Coltan in the mill; estimated up to 0.53 mSv (98 per cent of the total exposure) per annum on average. Further assessment of radiation exposure due to NORM should be carried out in the whole country and consider not only coltan but also other minerals of economic importance.

TABLE OF CONTENT

LIST OF TABLES

LIST OF ABBREVIATIONS AND SYMBOLS

1) ABBREVIATIONS

ADC: Analog to Digital Converter
AF: Absorbed Fraction
AEM: Analytical Electron Microscopy
AXIL: Analysis of X-ray spectra by Iterative Least-squares fitting
CA: Control Area
CDE: Committed Dose Equivalent
CIA: Central Intelligence Agency
DRC: Democratic Republic of Congo
DRF: Dose-Rate Factor
EC: European Commission
EDXRF: Energy Dispersive X-Ray Fluorescence
Euratom: European Atomic Energy Community
FWHM: Full Width at Half Maximum
GANAAS: Gamma Spectrum Analysis, Activity Calculations and Neutron Activation
                Analysis
HBRA: High Background Radiation Level Areas
HCA: Hierarchical Cluster Analysis
HLNBRA: High Level Natural Background Radiation Areas
IAEA: International Atomic Energy Agency
ICRP: International Commission on Radiological Protection
LDL: Lower Detection Limits
MAD: Maximum Annual Effective Dose
MCA: Multichannel Analyzer
NCRP: National Council on Radiation Protection
NORM: Naturally Occurring Radioactive Materials
PCA: Principal Component Analysis
PR :   Pattern Recognition
QXAS: Quantitative X-ray Analysis System
REDEMI: Régie d'Exploitation et de Développement des Mines
SEE: Specific Effective Energy
SSI: Swedish Radiation Protection Institute
TENORM: Technologically Enhanced Naturally Occurring Radioactive Materials
UNSCEAR: United Nations Scientific Committee on the Effect of Atomic Radiation
USEPA: United States Environmental Protection Agency

VHBRA: Very High Background Radiation Area
XRF: X-Ray Fluorescence

2) SYMBOLS

Au :   Gold
Be :   Beryllium
Bi :   Bismuth
Bq :   Becquerel
Br: Bromine
C: Celsius
Ca: Calcium
Cd: Cadmium
cm: Centimeter
Cs: Cesium
Co: Cobalt
Fe: Iron
g :   Gramm
Ga: Gallium
Gy :   Gray
h: Hour
J: Joule
K: Potassium
KeV   Kilo-electrovolt
kg :   Kilogramme
l: Liter
Li: Lithium
m :   Meter
MeV :   Mega-electrovolts
mg: milligram
ml: milliliter
Mn: Manganese
mSv :   millisilvert
Nb: Niobium
nGy :   Nano gray
Pb: Lead
Ra: Radium
Rb: Rubidium
Si: Silicon
Sn: Tin

Sr:	Strontium
Ta:	Tantalum
Th:	Thorium
Ti:	Titanium
U:	Uranium
y:	Year
Y:	Yttrium
Z :	Atomic number
Zn:	Zinc
Zr:	Zirconium
µg :	Microgramme
µSv :	Microsilvert
µCi :	Micro-curi

Chapter 1

1.0 INTRODUCTION

1.1 Introduction overview

Human beings are exposed to natural radiations arising from within and outside the Earth. The exposure to ionizing radiation from natural sources occurs because of the naturally occurring radioactive materials (NORM) in the soil and rocks, cosmic rays entering the Earth's atmosphere from outer space and the internal exposure from radioactive elements incorporated in food, water and air. Natural radioactivity is widespread in the Earth's environment and it exists in various geological formations in soil, rocks, plants, water and air (Ibrahiem *et al.*, 1993; Aly *et al.*, 1999; Malance *et al.*, 1996). In addition to NORM, some human activities e.g. medical diagnostic and therapeutic procedures, nuclear weapons production and testing, mining and milling of ores, extraction of petroleum products, use of groundwater for domestic purposes, nuclear power generation, accidents such as the one at Chernobyl in 1986, space travel and even living in houses could lead to enhanced exposure to natural sources of radiation. These are referred to as technologically enhanced naturally occurring radioactive materials (TENORM).

The total number of workers exposed to ionizing radiation (occupational exposure) is currently estimated to be about 22.8 million globally, of whom about 13 million are exposed to natural sources of radiation and about 9.8 million to artificial sources. The term workers means people who could be inadvertently exposed to ionizing radiation while at work. Medical workers comprise the largest proportion (75 per cent) of workers exposed to artificial sources of radiation (UNSCEAR, 2008).

Research on health risks associated to naturally occurring radioactive noble gas radon and its progenies has gained great attention, in particular those aspects related to controlling high radon concentrations (ICRP65, 1994; USEPA, 2004) and regulating the air quality in workplaces (SSI, 1999; Gooding et al., 1992; Risica, 2001). Since workers spend an average of approximately 2000 hours per year at their workplaces, the radiation exposure from radon in the workplace could be significantly high in cases where the radon concentration is relatively high (Sciver et al., 1995; Dixon et al., 1996; Jasim,1990, Eggermon, 1990).

Rwanda like many other developing countries doesn't have regulations for dealing with radiation exposures due to naturally occurring radioactive materials (NORM), but there are international (ICRP, 2000; AIEA, 2004) and national (NCRP, 1993) guidelines and directives with recommended limits for occupational exposures and for exposures to the public. Based on the risk factors, the International Commission on Radiological Protection (ICRP) has published recommendations for dose limits as follow: For occupational exposure the effective dose is limited to 20 mSv per year averaged over 5 years (100 mSv in 5 years) with the further provision that the effective dose should not exceed 50 mSv within any single year. For public exposure, the ICRP has recommended a limitation of the effective dose to 1 mSv per year. In special circumstances, however, a higher value may be allowed in a single year if the average over 5 years does not exceed 1mSv per year. The recommended dose limits by the National Council on Radiation Protection (NCRP) are identical to those of the ICRP for the most part. The cumulative effective dose for occupational exposures recommended by the NCRP is 10 mSv times the individual's age in years whereas the ICRP recommended value is 100 mSv over five years. For members of the public, the NCRP recommends an annual limit of 1 mSv, where exposure is continuous or frequent and 5 mSv where exposure is infrequent (NCRP, 1993). The above limits comprise the sum of internal and external exposures. The

term general public means specific individuals residing near areas or installations releasing radioactive materials into the environment.

The International Atomic Energy Agency (IAEA, 2004) and European Atomic Energy Community (Euratom) (EC, 2002) also recommend exemption levels in activity concentrations for substances containing NORM. The corresponding activity concentration exemption levels recommended by IAEA are 1, 1, 1, 10 Bq g^{-1} for ^{238}U, ^{226}Ra, ^{232}Th and ^{40}K respectively whereas those recommended by EC are 0.5, 0.5, 0.5 and 5 Bq g^{-1} for ^{238}U, ^{226}Ra, ^{232}Th and ^{40}K respectively. The exemption levels in activity concentrations for solid waste are derived from the following criteria: In normal circumstances, the effective dose of any member of the public is limited to 0.01mSv y^{-1} whereas in accidental situations, the effective dose may not exceed 1 mSv y^{-1}. For liquid and gases radioactive waste, the exemption levels are based on the individual dose limit of 1 mSv y^{-1}.

Gamma radiations are emitted from primordial radionuclides in soil and rocks and dominate the external radiation dose to the human body (UNSCEAR, 2000; Tzortzis *et al.*, 2004). Primordial radionuclides associated to external radiation are the ^{238}U (Uranium) radioactive decay series, ^{232}Th (Thorium) radioactive decay series and ^{40}K. Although the ^{235}U (Actinium) series also exists in soil, it accounts for a very small contribution to the human body exposure. Uranium-238 comprises 99.275 % of natural uranium in soil with a ^{235}U/^{238}U activity ratio of 0.04604 (Delko, 1996). The abundance of uranium and thorium varies widely over geographical areas. Igneous and sedimentary rocks on average contain concentrations on the order of 0.5 to 5 mg per kg of ^{238}U and 2 to 20 mg per kg of ^{232}Th. These correspond to radionuclide concentrations of about 6 to 60 Bqkg^{-1} of ^{238}U and 8 to 80 Bq of ^{232}Th (NCRP, 1988).

People involved with mining activities are exposed to NORM (Mustapha *et al.*, 2007, Lipsztein *et al.*, 2001, Banzi *et al.*, 1999). For example, in Eastern Democratic Republic of Congo, the occupational dose exposure due to grinding and sieving coltan is up to 18 mSv per annum on average (Mustapha *et. al.*, 2007).

In many parts of Rwanda, artisan miners extract and process columbite-tantalite from open pits manually and use very crude tools without any system of protection. In these processes (digging the coltan ore, sloshing the ore and soil in washtubs to separate coltan from soil, drying the coltan in open air, and finally grinding and sieving the dried coltan), the miners are susceptible to radiation exposures from naturally occurring radioactive series.

Miners may also experience internal exposures to radon, thoron (and their short-lived decay products) and other airborne radionuclides or those ingestible via dust as well as external exposures to gamma radiation from their surroundings. Figure 1.1 to 1.4 show workers engaged in various operations in a typical Ruli Coltan mining site.

Exposure of the general public living near the mines may arise from radionuclides which may be directly ingested through drinking contaminated water or through the food chain. Exposure of the public may also result from the reuse of the mine wastes (tailings and mine waters). Apart from the radiological problems, mining is also associated with other non-radiological problems such as toxic heavy metals, pollution and land degradation.

This study reports the occupational radiation doses and heavy metal fluxes from different working scenario received by mine workers in three regions of Rwanda: Muhanga, Ruli and Ngoma coltan mines.

Figure 1.1: Typical Ruli Coltan mining area

Figure 1.2: Artisan miners digging Coltan

Figure 1.3: Artisan miners washing Coltan

Figure 1.4: Artisan miners drying Coltan

Elemental analysis of coltan ore and mineral samples was determined by using the Energy Dispersive X-Ray Fluorescence (EDXRF) spectrometry. The activity concentration of primordial radionuclides ^{40}K, ^{238}U and ^{232}Th in samples of coltan, sediments and soil was determined by using hyper pure germanium (HPGe) based gamma-ray spectrometry, and the effective dose was derived from the activity concentration. Calculated effective dose and measured effective dose was compared in order to estimate the exact contribution dose from coltan mineral ore radionuclides.

Multivariate chemometric techniques via Principal Component Analysis (PCA) and Hierarchical Cluster Analysis (HCA) were used to compute, screen and display patterns and correlations in activity concentration and heavy metals elements graphically thereby showing possible groupings and sources of data variation.

1.2 Statement of the research problem

Because radioactive materials occur naturally throughout the Earth's crust, any mineral extraction operation or process has to be considered for radiological safety. There is, however, a general lack of knowledge of radiological hazards and exposure levels by all those concerned, including legislators, regulators, operators of workplaces as well as the workers due to the lack of baseline data which can inform decision making. There is also lack of regulatory framework for this type of exposure mainly due to inadequate research data to help inform policy. Many countries still do not have regulations for dealing with radiation exposures due to NORM, but information is available from international organizations to inform guidelines, directives and recommendations on how to mitigate against exposures of workers and the general public. This uncontrolled exposure is a health and ecological risk to

the people involved. In Rwanda like many African and developing countries hardly any research concerning NORM and radiological impact exposure associated with the extraction, processing and use of minerals especially columbite-tantalite has been carried out. Such a study, if undertaken, would provide sufficient information and data to make valid estimates of occupational radiation exposure and associated heavy metal fluxes in some mining areas of Rwanda.

1.3 Objectives of the research

The main goal of this study is to assess heavy metals fluxes and radiation exposure due to NORM in the mining and extraction of columbite-tantalite. The specific objectives are:

(i)   To measure the absorbed gamma dose rates in Muhanga, Ruli and Ngoma mining areas of Rwanda by using a gamma-ray radiation survey meter.

(ii)   To determine the activity concentrations of the naturally occurring radionuclides (^{40}K, ^{226}Ra, ^{232}Th) in the coltan ore, soil, and mine sediment samples.

(iii)   To derive from (ii) above the absorbed dose rates in air and the external and internal exposure of people to terrestrial gamma rays from the primordial radionuclides in coltan ore, soil and mine sediments.

(iv)   To measure the concentration of heavy metals in coltan ores, sediments and soil samples from these areas.

(v) To explore the multivariate relationships between the measured quantities using Pattern Recognition (PR) techniques such as Principal Component Analysis (PCA) and Hierarchical Cluster Analysis (HCA) and utilize the data above to assess the comparative quality associated with Rwandan coltan.

1.4 Justification and significance of the research

The benefits to be derived from radiological survey of exposure to artisans mining columbo-tantalite (coltan) in Muhanga, Ruli and Ngoma areas of Rwanda include the following:

(i) Data produced on exposure levels will serve as information for awareness among the legislators, regulators, operators of work places, the artisans, and the general public about the potentials of radiological exposures due to presence of NORM in the coltan mining material.

(ii) Results obtained, using chemometric techniques (PCA and HCA) may be applied to obtain a quality assessment model for coltan mining in Rwanda.

(iii) Heavy metals analysis will identify, toxic metals pollutants to which artisan miners are exposed to, those which are normally associated with coltan, and radiological elements associated with coltan minerals.

(iv) These data will form the baseline background data for further studies on assessment of radiation protection and its radio–ecological impact in Rwanda.

8

1.5 Expected outcome

Artisans involved with extracting, processing and using Coltan in Eastern Democratic Republic of Congo are potentially at risk of high occupational exposure to NORM (Mustapha *et al.*, 2007). Since the eastern Democratic Republic of Congo shares the same geological features as those of Rwanda, it is expected that the Rwandan mine workers face the same problem.

Chapter 2

2.0 LITERATURE REVIEW

2.1 General geology of Rwanda

Rwanda is a landlocked mountainous country in Eastern Africa. The landscape of this 'Land of a Thousand Hills' is characterized by rolling highlands in the central and eastern part of the country and rift-valley related volcanic mountains and rift lakes in the west and northwest. The geology of Rwanda is similar to the geology of neighbouring Burundi and southern Uganda. The oldest rocks of Rwanda are migmatites, gneisses and mica schists of the Paleoproterozoic Ruzizian basement overlain by the Mesoproterozoic Kibaran Belt (Thomas, 2008). The Kibaran Belt, composed of folded and metamorphosed sediments, mainly schists and quartzites intruded by granites, covers most of Rwanda. This belt is known to be largely mineralised. The phenomenon explains the occurrence of various mineral deposits in the country.

In the east of the country predominate older granites and gneisses. Cenozoic to recent volcanic rocks occur in the northwest and west of the country. Some of these volcanoes are highly alkaline and are extensions from the Virunga volcanic area of southwestern Uganda and eastern Democratic Republic of Congo. Tertiary and Quaternary clastic sediments fill parts of the Western Rift in the western part of the country. Young alluvials and lake sediments occur along the rivers and lakes. Figure 2.1 describes the general geology of Rwanda.
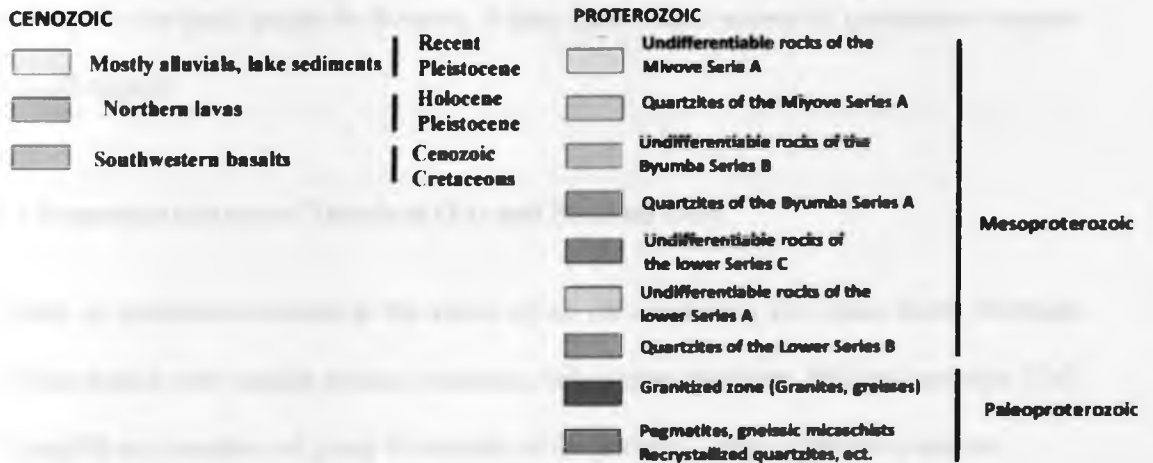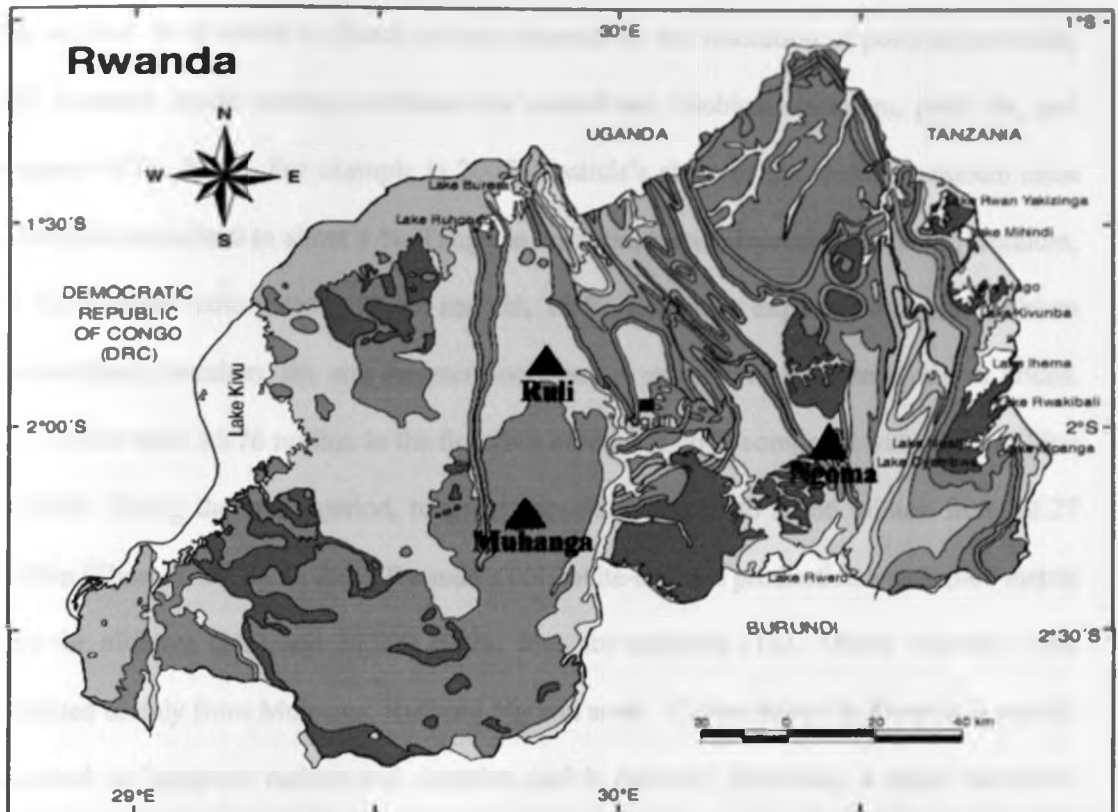
Figure 2.1: Geological map of Rwanda (Thomas, 2008).

2.2 Minerals of Rwanda

The most exploited minerals are cassiterite, wolfram and columbo-tantalite (coltan). Other minerals such as gold, beryl, amblygonite, iron, ruby/sapphire, chiastolite, amethyst, marble, dolomite, laterite, e.t.c. are mined to a lesser extent.

11

The outlook for Rwanda's mineral industry depends on the resolution of political instability and favorable world market conditions for columbium (niobium)-tantalum, gold, tin, and tungsten (CIA, 2000). For example in 2007, Rwanda's share of the world's tantalum mine production amounted to about 4 %. Tungsten mine production increased by 87 %, tantalum, 32 %; niobium (columbium), 29 %; and tin, 19 %. Rwanda's exports earning of niobium (columbium), tantalum, tin, and tungsten increased in early 2007 because of higher prices. Tin exports were $6.76 million in the first four months of 2007 compared with $3.39 million in 2006. During the same period, tungsten exports increased to $7.66 million from $2.27 million (Thomas, 2008). In 2007, Rwanda's columbite-tantalite production was 80,000 metric tons for niobium (Nb) and 50,000 metric tons for tantalum (Ta). Theses minerals were extracted mainly from Muhanga, Ruli and Ngoma areas. Coltan mined in Rwanda is mainly exported to European nations and America and is currently becoming a major economic activity for the local people in Rwanda. It also forms major source of government revenue through export.

2.3 Properties and use of Tantalum (Ta) and Niobium (Nb)

Coltan or columbite-tantalite is the name of an ore containing two Rare Earth Elements (REEs) metals with similar atomic structures; columbium (niobium, Nb) and tantalum (Ta). Ta and Nb are members of group V elements in the periodic Table i.e transition metals.

Tantalum (Ta) is a rare, grey-blue metal, atomic number 73, which occurs in over 100 minerals as the oxide, Ta_2O_5. The most common form is "tantalite". It is found with other elememts such as tin, lithium, titanium, thorium and uranium. Its melting (2,996 °C) and boiling (5,425 °C) points confer significant heat resistance. It is also highly resistant to corrosion and almost completely immune to chemical attack at temperature below 150 °C. Tantalum is as twice dense as steel and highly durable. It is also highly ductile and surpasses

most other refractory metals in workability and weldability. Other properties are superconductivity and a high co-efficient of capacitance, which means that it can store and release an electrical charge (Karen, 2003, Roskill, 2002). Tantalum capacitors are used in mobile phones, video cameras, note book computers, pagers, automotive electronics and playstations where they buffer and smooth the flow of electricity. High corrosion resistance makes tantalum an ideal material in the fabrication of chemical process equipment, heat exchanges, instrument protection devices, reactor lining, laboratory ware and prosthetic devices.

Niobium is a shiny gray metal with a melting point of 2,468 °C and a boiling point of 4,927 °C. Its density is 8.57 g cm^{-3}. Niobium metal is resistant to attack by most common chemicals. It does not combine with oxygen or most other active elements except at high temperatures. It does not react with most strong acids unless they are hot and concentrated. Niobium is used primarily in making alloys. For example, the addition of niobium to steel at very high temperature greatly increases its strength (Gupta, 1994). Such steel are used in the construction of nuclear reactors, airplanes, space vehicles and superconducting magnets. Niobium alloys are also used in items that come into contact with the human body, such as rings for pierced ears, nose, and other body parts. Niobium is used in this kind of jewelry because it does not cause allergies or other problems.

2.4 High background radiation areas (HBRA)

According to the United Nations Scientific Committee on Effects of Atomic Radiation Report (UNSCEAR, 2000), the greatest contribution to the mankind's exposure comes from natural background radiation, and the worldwide average annual effective dose is 2.4 mSv. However, around the world there are some areas having elevated natural background radiations; these

areas are known as High Background Radiation Areas (HBRA). Such areas include, Lambwe and Mrima hill in Kenya , Ramsar in Iran, Guarapari in Brazil, Kerala in India, the northern Flinders Ranges in Australia and Yangjiang in China.

A radiological survey by Achola (2009) of the various parts of Lambwe east location (South western Kenya) indicated that the mean estimated annual external effective dose rate due to radionuclides in rocks and soil was 5704.78 μSv y^{-1}. The average specific activity concentrations of potassium-40, Radium-226 (uranium-238 equivalent) and thorium-232 in rock and soil samples from these areas were measured to be 508.67 Bq kg^{-1}, 178.69 Bq kg^{-1} and 1396.85 Bq kg^{-1} respectively using gamma-ray spectrometry. The study indicated that the source of enhanced level of natural radioactivity in the sample was mainly carbonitite rocks. Based on the higher levels of gamma-absorbed dose rates in air (5.705 mSv y^{-1}) as compared to the global mean of 0.46 mSv y^{-1}, this region was characterized as high natural background radiation area (HBRA).

Similar results have been reported in other parts of Kenya such as Mrima hill (Mangala, 1987; Patel, 1991; Mustapha, 1999); Ruri hills, Rangwa ring complex, Soklo point and Kuge (Tuinge), in Gwasi, Suba district (McCall, 1958). Thorium, niobium, lead, strontium, zinc were found in high concentration in the soil and rocks samples from Mrima Hills (Mangala, 1987). Thorium and traces of rare earth metals were also found in high concentrations (> 1000 μg g^{-1}). The survey by Patel (1991) indicated that Mrima hills area is composed of deeply weathered carbonites rock and has high natural radioactivity (HBRA). The upper and lower levels of external gamma radiation doses were 106.7 mSv and 1.372 mSv respectively. These levels were estimated to be approximately 50 times more than the ones from normal natural background doses. The author recommended that sedimentary rock from the hill

should not be used either for building houses or road construction or any other similar purposes and water from the bore-holes at the base of the hill should be tested for radioactive contamination because oxides of thorium and rare-earths are soluble. Water samples from some public wells in Mrima were tested by Mustapha (1999) and showed radon levels around 100 kBq m^{-3}. This was attributed to occurrences of thorium enriched carbonatite rocks in the area.

The highest levels of natural background radiation recorded in the world to date is from areas around Ramsar, particularly at Talesh-Mahalleh which is considered to be a very high background radiation area (VHBRA) having an effective dose (260 mSv y^{-1}) equivalent to 13 times in excess of ICRP-recommended radiation dose limits for radiation workers (20 mSv y^{-1}), 260 times higher than the effective dose recommended by ICRP to the general public, and up to 108 times greater than normal background levels (Ghiassi-nejad, 2002). Most of the radiation in the area is due to dissolved ^{226}Ra in water of hot springs along with smaller amounts of Uranium and Thorium due to travertine deposits.

The abnormally high terrestrial gamma radiation in Brazil is due to the presence of monazite sand along the Atlantic coast and volcanic intrusion in the state of Minas Gerias. Dose rate in this area ranged up to 2.1 Gy h^{-1} (Malanka et al., 1993). Similar results were observed in Kerala, India. The environmental radiation emanates largely from the thorium deposited mostly along coastal areas. The average dose received by the population is about 4 times the normal background radiation level, and the dose rate varies from 1 to 45 mGy h^{-1}. In certain locations on the coast, it is as high as 70 mGy y^{-1} and on average is 7.5 times the level seen in interior areas (Chougaonkar et. al., 2003).

In the case of Yangjiang, Guangdong province (China), the sources of background radiation were nearby mountains whose surface rocks were found to be granites from which fine particles of monazite were washed down continuously year by year by rain and deposited in the surrounding basin region resulting in the elevation of the levels of the background radiation (Wei, 1980). The results of the analyses of soil samples by gamma-ray spectrometry and radiochemistry as well as the measurements of field gamma spectrometry showed that the concentrations of natural radionuclides in soil were quite different between the two areas designated as high level natural background radiation areas (HLNBRAs) and control area (CA), especially that of thorium which was about six times higher in high level natural background radiation area than that in control area.

High radiation above the global average is mainly due to naturally occurring radiation radioactive elements in the earth crust such as ^{238}U, ^{232}Th and ^{40}K. Areas at high altitudes are also affected by cosmic radiations (NCRP, 1987; UNSCEAR, 1993; Bennett, 1997).

Hitherto, no research concerning NORM and occupational radiation exposure in the mining industry has been carried out in Rwanda. Rwanda is suspected to be a HBRA because it's geological features. The most predominates rocks of Rwanda are granites and these are known to be associated with higher radiations levels (UNSCEAR, 2000).

2.5 Radiation exposure due to NORM in mining areas

Mining work activities associated to mineral extraction, processing of minerals with naturally radioactive materials (NORM) which have the potential to cause exposures to radiation and toxic heavy metals to members of the general public and workers. This is due to the industrial, physical, chemical and thermal processes which disturb the natural equilibrium of

the radionuclides and resulting in an enrichment of some radionuclides compared to the original matrix.

Over the years measurement of radioactivity and assessment of occupational exposure of radiation to workers and the general public in different parts of the world has been studied. Some of these studies are presented in the following sections.

Funtua and Elegba (2005) estimated the radiological impact of the processing of cassiterite and columbite from different mills of Jos Plateau (central Nigeria). The results indicated that the average dose rate at different processing points and locations at the mills had values ranging from 5 μSv h^{-1} to 80 μSv h^{-1} for the background radiation in the premises and processed zircon respectively. Assuming a 2000 h working year, workers in the processing mills were exposed to an annual dose of about 10 mSv for the background and an average of 160 mSv for processed zircon, far above the 20 mSv annual dose limit. The dose rates of about 25 μSv h^{-1}, measured from the tailings, gave an annual dose of about 50 mSv for a non-radiation worker in the vicinity of the milling plant, exceeding the recommended 1 mSv y^{-1} dose limit for the members of the public. The authors concluded that there were high-level radiation exposures (mainly of Th series) from the mine tailings of Jos area, central Nigeria.

A similar related study was carried out by Odumo (2009) in the artisanal gold mining belt of south-western Nyanza (Kenya). The average activity concentration of ^{40}K (100 Bq kg^{-1}), ^{226}Ra (25 Bq kg^{-1}) and ^{232}Th (41 Bq kg^{-1}) were in this case however found to be below the global average. ^{226}Ra in the examined mine water samples was found to be below the detection limit (0.94 kBq m^{-3}). The dust loading at the crushing sites was examined; the upper and lower levels of dust loading were 3.668 mg m^{-3} and 1.334 mg m^{-3} respectively. The

average absorbed dose in air due to gamma – ray emitters in the mines was found to be lower (42 nGy h^{-1}) than the world average outdoor exposure value of 55 nGy h^{-1}. The annual effective dose in the mines is below 1 mSv y^{-1} and 20 mSv y^{-1}, the limits for the general public and radiation worker respectively. Among the working scenarios, crushing had the highest potential of exposure scenario and the highest exposure pathway was the inhalation of contaminated dust. High levels of well known toxic elements such as arsenic (3274 mg kg^{-1}), lead (1413 mg kg^{-1}) and zinc (587 mg kg^{-1}) were also recorded in the study.

A study on the activity and ambient background radiation in the Majingu phosphate mine in Tanzania found high concentration of ^{226}Ra in phosphate rock (5,760±107 Bq kg^{-1}) and waste rock (4,250±98 Bq kg^{-1}) while surface waters had an activity concentration of 4.7±0.4 Bq l^{-1} (Banzi et al., 1999). The authors also found that the absorbed dose rate in air range from 1375-1475 nGy h^{-1} (average: 1415 nGy h^{-1}). This average is 28 times that of the global average background radiation from terrestrial sources, and about 12 times the average dose limit for public exposure recommended by ICRP.

Comparison of the findings of Elegba (2005) and Odumo (2009) shows that work activities related to the mining and processing of cassiterite and coltan enhance more the levels of radiations exposure than works related to the mining and processing of gold.

A pilot survey program, that included six mines in Brazil (two coal, one niobium, one gold and one phosphate mine), was launched in order to determine the need to control the radioactive exposure at mine workers (Lipsztein et. al., 2001). The survey consisted of the analysis of uranium, thorium and polonium in excreta samples of workers, family members

of the workers and residents from the general population of Rio de Janeiro. The survey consisted also of measuring thorium and uranium in air samples. The results from the coal mines indicated a daily intake of uranium that varied 0.2-0.58 Bq. The committed effective and the annual effective doses due to uranium for coal mine workers and their dependant were very low. There is no enhanced internal contamination due to radioactive elements in the nickel, phosphate, and the gold mines that were surveyed. The niobium mine results showed the in some areas of the industry exposure to thorium and uranium might occur. The authors indicated that there might be a need for a program to control radon exposures in the coal mines and for a control of radon exposures and thorium in the niobium mine.

Analysis of columbite-tantalite from Eastern Democratic Republic of Congo by Mbuzukongira (2006) indicated that the most abundant elements in the samples were Sn, Ta, Nb and Fe. The concentration range was estimated as; (131.6-464.0) mg g^{-1} for Sn, (144.1-340) mg g^{-1} for Ta, (17.2-123.7) mg g^{-1} for Nb, and (40.4-100.4) mg g^{-1} for Fe. The other elements that were found in concentrations higher than 10 mg g^{-1} were Mn, Ca, Ti and Au. These results classify coltan from this part of DRC as a tantalite because tantalum is more abundant.

Gamma-ray spectrometry was used to analyze activity concentrations of ^{226}Ra and ^{232}Th in processed coltan, extracted coltan, sediments and soil samples. In most of the samples, ^{40}K was not detected above the detection limit which was calculated to be 0.141 Bq g^{-1}. The average activity concentrations of ^{226}Ra and ^{232}Th were 7.06 Bq g^{-1} and 1.75 Bq g^{-1} respectively. These values are much higher than the world wide average values (i.e 0.035 Bq g^{-1} for ^{226}Ra and 0.030 Bq g^{-1} for ^{232}Th) reported by UNSCEAR (2000). The author

concluded that the coltan ore contains enhanced levels of natural radioactivity as a result of mining process.

Effective and total dose to miners due to digging coltan were calculated and found to vary 0.007-18.1 mSv y^{-1}. These values depend on the various mining activities, but crushing and sieving of coltan in the mills resulted in the highest exposure dose. The most significant pathway of exposure to radionuclides was the inhalation of Coltan bearing dust, and the least significant was the external exposure from submersion in Coltan contaminated air. The author concluded that there was urgent need to reduce these levels of exposure, for example by shielding the stockpiles of coltan and by introducing dust control measures. It was also recommended that field measurement should be carried out in future research to validate calculated results presented in the report.

The present study has assessed exposure by comparing both field measurements values and those calculated by adopted model. Data was analyzed by using chemometric techniques such as Principal Components Analysis and Hierarchical Cluster Analysis (HCA) in addition.

3.0 THEORY

3.1 Introduction

When gamma radiation is transmitted through matter, it produces various interactions that deposit energy in the medium. Knowledge of the basic physics of radiation interaction and energy transfer is fundamental to radiation detection, measurement, and control, as well as to understanding the biological effects of radiation on tissue. The goals of this chapter are i) to describe radiation interaction processes ii) to apply these concepts to radiation detection and the calculation of deposited energy, i.e., radiation exposure and dose. The principal modes by which photons interact with matter are the photoelectric effect, the Compton effect, and pair production. Photoelectric interactions are dominant at low energies and pair production at high energies, with Compton scattering being dominant in the mid-energy ranges (Figure 3.1).
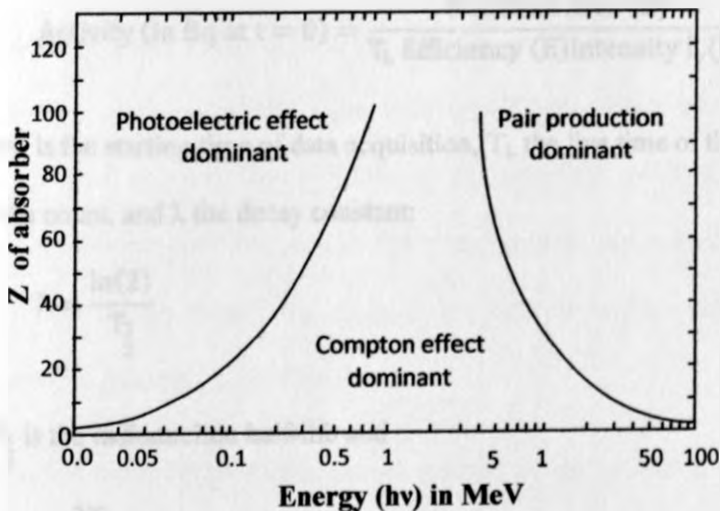
Figure 3.1: The three major types of gamma-ray interaction with matter (Knoll, 1997).

Photons also undergo Rayleigh scattering, Bragg scattering, photodisintegration, and nuclear resonance scattering; however, these result in negligible attenuation or energy deposition and can generally be ignored for most purposes of radiation protection (Gordon, 2008).

3.2 Theory of gamma ray spectroscopy

When the sample to be analyzed is placed on the detector, the gamma rays (energy) produced from the radionuclides present in the sample interact with the detector crystal via one of the three processes; photoelectric effect, Compton effect, and pair production (Michael, 2003; Knoll, 1997; Crouthamel, 1975). Any interaction deposits energy and generates electrons creating electron-hole pair in the detector. The quantity of charge produced is directly proportional to the energy of the incident photon. The electric charge (electron-hole pair) within the detector active volume is released as pulses and viewed as peaks (pulse height). From these pulses one can infer the type of radiation being detected.

The activity of a sample is calculated in gamma spectrometry from the following equation (Michael, 2003):

$$\text{Activity (in Bq at t = 0)} = \frac{\text{Net Peak Area (E)}}{T_L \text{ Efficiency (E)Intensity } I_\gamma(E)} \frac{\lambda T_R}{1 - e^{-\lambda T_R}} \quad (3.1)$$

where t=0 is the starting time of data acquisition, T_L the live time of the count, T_R the real time of the count, and λ the decay constant:

$$\lambda = \frac{\ln(2)}{T_{\frac{1}{2}}} \quad (3.2)$$

where $T_{\frac{1}{2}}$ is the radionuclide half-life and

$$\frac{\lambda T_R}{1 - e^{-\lambda T_R}} = \text{decay correction for decay during the counting period} \quad (3.3)$$

This correction factor converts the nominal count rate (Peak Area/T_L) to the count rate at time t= 0

$$\text{Intensity } I_\gamma(E) = \frac{\text{gamma emission rate (at energy E)}}{\text{disintegration rate}} \qquad (3.4)$$

and

$$\text{Efficiency (E)} = \frac{\text{full-energy deposition rate (at energy E)}}{\text{gamma emission rate (at energy E)}} \qquad (3.5)$$

The efficiency expresses the relationship between the full-energy deposition rate and the emission rate of the sample.

3.3 Theory of X-Ray Fluorescence (XRF) spectroscopy

The X-ray fluorescence process is initiated by an ejection of an electron by photon energy that creates an electron vacancy in the atom. This vacancy is filled by transition of an electron from the outer shell. The difference in binding energies of the two electrons results in the creation of characteristic X-rays. The excitation energy from the inner atom may also be transferred to the outer electrons causing it to be ejected from the atom, such an electron is called Auger electron. Because each atom has a unique orbital structure, then the resulting characteristic X-rays are also unique with specific frequency and act as fingerprints of elements in XRF analysis. The emission of characteristic radiation can be induced by the impact of accelerated particles such as electrons, protons, alpha particles and ions; or by the impact of high energy radiation from an X-ray tube or suitable radioactive source. In this work, cadmium (Cd-109) source was used.

By measuring the X-ray radiation energy emitted by the sample it is possible to determine which elements are present. This step is called qualitative analysis. By measuring the

intensities of the emitted fluorescence radiation it is possible to determine how much of each element is present in the sample. This step is called quantitative analysis (Brouwer, 2003).

The elemental concentration was evaluated using Sherman's equation (IAEA, 2005);

$$I_i(E_i) = G_o.K_i.\varepsilon(E_i).\rho_i d_i \left[\frac{1 - \exp(-a\rho d)}{a\rho d} \right] \qquad (3.6a)$$

where

$I_i(E_i)$ is the measured fluorescent intensity of element i.

$I_o(E_o)$ is the intensity of primary exciting radiation.

G_o is the geometry constant which is also dependent on the source activity as is

the case with radioisotope sources.

$$G_o = \frac{I_o(E_o)\Omega_1\Omega_2}{\sin\phi_1} \text{ in which}$$

Ω_1 is the solid angle of the incident primary radiation as seen by the sample.

Ω_2 is the solid angle of the emergent secondary radiation as seen by the detector.

K_i is the relative excitation efficiency given by;

$$K_i = \sigma_i^{ph}(E_O).(1 - 1/J_{is}).\omega_{is}.f_s^i \text{ in which}$$

$\sigma_i^{ph}(E_o)$ is the photoelectric mass absorption coefficient of element i at energy E_o

ω_{is} is the fluorescence yield for element i in shell "s".

$(1 - 1/j_{is})$ is the relative probability for photoelectric effect in shell "s".

f_s^i is the ratio of the intensity of a given K or L line to the intensity of the whole

series.

$\rho_i d_i$ is the mass per unit area of element i in the sample.

d is the thickness of the sample and ρ its density.

$\varepsilon(E_i)$ is the relative efficiency of the detector for photons of energy E.

The total mass absorption coefficient for primary and fluorescent X-ray radiation in the sample is given by

$$a = \mu(E_o)\csc\phi_1 + \mu(E_1)\csc\phi_2, \text{ in which}$$

$\mu(E_o)$ and $\mu(E_1)$ are the total mass absorption coefficients in the sample at

primary and secondary energies.

ϕ_1 is the incident angle of primary radiation with the sample.

ϕ_2 is the emergent angle of secondary radiation with the sample.

In the derivation of equation 3.6a, the following assumptions were made;

(i) The excitation source is considered to be a point source.

(ii) The sample is homogeneous.

(iii) The primary radiation is monochromatic.

(iv) The density of element i, ρ_i in the sample is constant over the whole sample volume.

(v) A fixed geometry is maintained during the intensity measurements of element i in the sample, thus ϕ_1 and ϕ_2 are constant and the detector is far from the sample.

The expression $\left[\dfrac{1-\exp(-a\rho d)}{a\rho d}\right]$ in equation 3.6a is called the absorption correction factor

and it accounts for the attenuation of the primary and secondary radiation in the sample.

For thin samples, approximation on the exponential term,

$\exp(-a\rho d) \approx 1 - a\rho d$, with a relative error of 1% for $a\rho d \angle\angle 0.01$ is assumed. Thus, equation 3.6a reduces to:

$$I_i(E_i) = G_o.K_i.\varepsilon(E_i)\rho_i d_i \tag{3.6b}$$

in which $\rho_i d_i \le \dfrac{0.134}{a\rho d}$. In this case the concentration in terms of the mass per unit area of

element i, is linearly dependent on the fluorescence radiation intensity.

For thick samples, approximation to $\exp(-a\rho d)$ in equation (3.6a), asymptotically tends to zero, for $a\rho d \gg 1$. Thus, equation (3.6a) reduces to;

$$I_i(E_i) = \frac{G_o.K_i.\varepsilon(E_i).\rho_i d_i}{a\rho d} \tag{3.6c}$$

in which $\exp(-a\rho d) < 0.01$, where $\rho_i d_i \geq \dfrac{0.461}{a\rho d}$ with relative error of 1%.

Practically I_i is obtained by using the software AXIL-QXAS.

3.4 External radiation exposure from radionuclides in soil

Assessment of exposure is extremely complex due to the large number of environmental factors which affect the gamma photon flux in air. The characteristics and the properties of the soil are the most relevant factors to determine the energy and the angular distribution of gamma radiation in air 1 m above the ground level. Calculations are based on the point-kernel integration method and assume that the source concentration at any depth in soil is uniform over an infinite surface parallel to the ground plane. The dose-rate factor is applied to environmental dose exposure assessments by means of the general equation (Kocher *et al.*, 1985):

$$H(t) = \chi(t) \times DRF \tag{3.7}$$

where, H is the external dose rate at time t, χ is the source concentration at the location of the exposed individual, and DRF is the dose-rate factor based on the consideration of the exposure to the torso of a standard man. In this case the torso is estimated to be at 1m above the ground.

The methods used to calculate the dose-rate factors involve idealized assumptions concerning vertical and lateral distributions of radiation sources in soil and the extent of shielding

provided by the air above ground. Undoubtedly these assumptions are not strictly valid for most realistic exposure situations. The geometry adopted for calculations of primary photon fluence is based on two semi-infinite volumes of soil and air separated by an infinite plane soil surface (Figure 3.2).
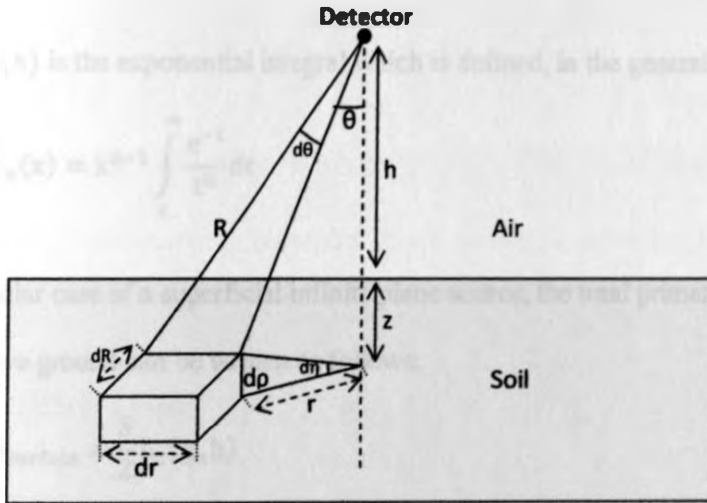
Figure 3.2: The geometry used in deriving the photon fluence from radionuclides in the ground (Source: Kocher *et al.*, 1985)

A photon source element is contained in a volume element $dV = drdRd\rho$ of soil at depth z below the soil surface. If the photon source is represented by $S(z,r,\eta)$ photons emitted per unit volume of soil as a function of depth z, lateral distance r and azimuthal angle η, then the primary photon fluence at the position of a hypothetical detector at height *h* above ground and at distance R from this volume element is:

$$d\Phi = \frac{S(z, r, \eta)dV \exp\left(-\mu_S(R - h\sec\theta) - \mu_a(h\sec\theta)\right)}{4\pi R^2}$$ (3.8)

where θ is the angle between the direction to the volume element and the normal to the air-soil interface, μ_S and μ_a are the mass attenuation coefficients for soil and air respectively.

The total primary photon fluence can be obtained by integrating equation 3.8 over the entire photon source in the soil. If we assume a uniform source distribution S, with infinite depth and infinite lateral extent in the ground, the primary photon fluence is

$$\Phi_{uniform} = \frac{\frac{S}{\rho_S}}{2\mu_S} E_2(\mu_a h) \tag{3.9}$$

where $E_2(\mu_a h)$ is the exponential integral which is defined, in the general case, as:

$$E_n(x) = x^{n-1} \int_x^\infty \frac{e^{-t}}{t^n} dt \tag{3.10}$$

In the particular case of a superficial infinite plane source, the total primary photon fluence at height h above ground can be written as follows:

$$\Phi_{surface} = \frac{S}{2} E_1(\mu_a h) \tag{3.11}$$

In equation 3.11, E_1 is the exponential integral of first order. The source concentration as a function of depth in soil in a determined time is given by:

$$S(z) = S(0) \exp(-\alpha z) \tag{3.12}$$

where $S(0)$ is the concentration at the ground surface, α is the reciprocal of the relaxation length and it depends on the radionuclide, the soil type and time after deposition. Operating adequately it is possible to obtain the following expression for the total primary photon fluence:

$$\Phi_{exp} = \frac{S(0)/\rho_S}{2\mu_S/\rho_S} \exp\left(\frac{(\alpha/\rho_S)\mu_S h}{\mu_S/\rho_S}\right)\left[F_1\left(\infty, \frac{-\alpha/\rho_S}{\mu_S/\rho_S}\right) - F_1\left(\mu_S h, \frac{-\alpha/\rho_S}{\mu_S/\rho_S}\right)\right] \tag{3.13}$$

In this equation the depth has been expressed in mass per unit area ($\rho_S z$) and the function $F_n(t,\alpha)$ is defined as:

$$F_n(t, \alpha) = \int_0^t \exp(\alpha y) \, E_n(y) dy \tag{3.14}$$

The absorbed dose results from the sum of individual contributions of each photon arriving to the receptor, according to the following equation:

$$D = \sum_{i=1}^{N} \Phi(E_i) \cdot \left(\frac{\mu_{ab}(E_i)}{\rho}\right)_{air} \cdot E_i \tag{3.15}$$

where, $D(Gy)$ is the absorbed dose in air, $\Phi(E_i)$ (Jm^{-2}) is the photon fluence with energy E_i, and $\left(\frac{\mu_{ab}}{\rho}\right)$ $(m^2 g^{-1})$ is the energy absorption coefficient in air for energy E_i.

3.5 Internal radiation dose

Internal radiation dose can occur due to inhalation or ingestion of radionuclides. All internal radiation dose determinations involve three quantities: (a) the total number of transformations that occur following the deposition of radionuclide in a source organ, the total number of transformations is a function of the activity of the deposited radionuclide and the time it remains in the source organ (b) the amount of energy (MeV) deposited per gram of target tissue for each transformation that occurs in a source target (c) a constant to adjust the units.

3.5.1 Absorbed dose in tissue

The internal radiation dose calculations are based on the assumption that the deposited radionuclide (expressed as its activity q in μCi or Bq) is uniformly distributed throughout the tissue mass of a source organ. Secondly, the internal radiation dose depends on the absorbed fraction AF (T←S). This parameter is the fraction of energy absorbed in a target organ T per emission of radiation from activity deposited in the source organ S. Since many radionuclides

produce more than one form of radiation emission per transformation, it is necessary to account for the energy absorbed due to each emitted radiation and its fraction Y_i of the number of transformations that occur. If the transformation rate q (t) of a radionuclide uniformly deposited in a tissue mass m_T is in Bq, the energy deposition rate per transformation is :

$$\dot{D}\left(\frac{erg}{g\,s}\right) = 1.6022 \times 10^{-6} q(t) \frac{\sum Y_i \bar{E}_i AF\,(T \to S)_i}{m_T} \qquad (3.16)$$

where q(t) = activity (Bq) of the radionuclide in the tissue at any time t, Y_i = fractional yield per transformation of each radiation emitted, $\bar{E}_i$ = average energy (MeV) of each emitted radiation, $AF(T{\leftarrow}S)_i$ = fraction of energy emitted by a source tissue S that is absorbed in a target tissue T, and m_T = mass (g) of target tissue T. This expression yields the "instantaneous" energy deposition (or dose) rate; it is a direct function of the amount of activity q(t) that exists at any time t in a source organ.

3.5.2 Accumulated dose

Although the "instantaneous" dose rate is of some interest, it is the accumulation of dose delivered over a period of time (usually the total dose) that is of most importance. All of the parameters that determine the instantaneous dose rate are constant for a given exposure situation except q(t) which varies with time after deposition in an organ due to the combined effects of radioactive transformation (physical loss) and biological turnover. The dose will diminish with time as shown in Figure 3.3 as a function of q(t),
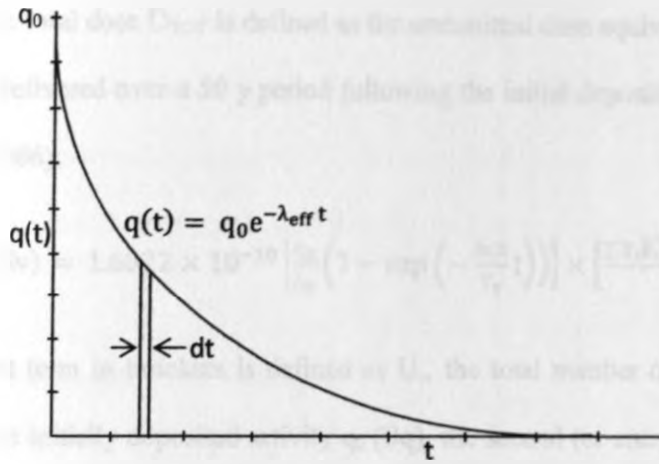
Figure 3.3: Variation of the instantaneous dose rate with time after deposition in a tissue (Martin, 2006).

The accumulated radiation dose is obtained by integrating the instantaneous dose rate equation from the time of initial deposition $(t = 0)$ in the tissue to a later time t. If the initial activity deposited in a source organ S is q_0, the total energy deposition (erg/g) in a target tissue T is:

$$D_{TOT} = 1.6022 \times 10^{-6} \frac{\sum Y_i \bar{E}_i AF\ (T \rightarrow S)_i}{m_T} q_0 \int_0^t e^{-\lambda_{eff} t}\ dt \qquad (3.17)$$

λ_{eff}, is a constant which depend on the effects of radiation transformation in an organ. After integration, the total energy deposition is:

$$D_{TOT} \left(\frac{erg}{g}\right) = 1.6022 \times 10^{-6} \left[\frac{q_0}{\lambda_e}\left(1 - \exp\left(-\frac{\ln 2}{T_e} t\right)\right)\right] \times \left[\frac{\sum Y_i \bar{E}_i AF\ (T \rightarrow S)_i Q_i}{m_T}\right] \qquad (3.18)$$

where the first term in brackets represents the total number of transformations that occur for a time t following the initial deposition of an activity q_0; the second term is the energy deposition (or dose) per transformation (erg g^{-1} t) in the tissue mass m_T; and the constant accounts for the units. D_{TOT} can also be expressed as J kg^{-1} by multiplying by 10^{-7} J erg^{-1} and 10^3 g kg^{-1}.

In SI units, the total dose D_{TOT} is defined as the committed dose equivalent, $H_{50,T}$, in units of sieverts (Sv) delivered over a 50 y period following the initial deposition of an activity q_0 in Bq (Martin, 2006):

$$H_{50,T}(Sv) = 1.6022 \times 10^{-10} \left[\frac{q_0}{\lambda_e}\left(1 - \exp\left(-\frac{\ln 2}{T_e}t\right)\right)\right] \times \left[\frac{\sum Y_i \overline{E_i} AF(T \rightarrow S)_i Q_i}{m_T}\right] \qquad (3.19)$$

where the first term in brackets is defined as U_s, the total number of transformations that occur due to an initially deposited activity q_0 (Bq), the second (or energy deposition) term in brackets is defined as the specific effective energy (SEE) with units of MeV t^{-1} g adjusted by the quality factor Q_i for each form of emitted radiation, and the constant 1.6×10^{-10} converts MeV t^{-1} g to J kg^{-1} t to yield, in Sieverts (Sv), the 50 years committed dose equivalent (CDE) in SI units; or

$$H_{50,T}(Sv) = 1.6 \times 10^{-10} U_s \times SEE(T \leftarrow S) \qquad (3.20)$$

U_s is calculated from an initially deposited activity of q_0 (Bq) where T_e is in seconds.

Since $\lambda_e = \ln 2/T_e$, it is

$$U_S(\text{no. of transformations}) = 1.443 \, q_0 T_e \left[1 - \exp\left(-\frac{\ln 2}{T_e}t\right)\right] \qquad (3.21)$$

The exposure period for a radionuclide deposited in a tissue is usually assumed to be 50 years, or a working lifetime, which is much longer than biological clearance for most radionuclides. Thus the total number of transformations that occur in an organ due to an uptake q_0 reduces to

$$U_s \text{ (no. of transformations)} = 1.443 q_0 T_e \qquad (3.22)$$

with an error of less than 1 % for exposure times that are 7–10 times the effective half-life T_e. Thus, this simplified expression of the total number of transformations can be used for internal dose calculations if, and only if, the integrated period of exposure is 7–10 times greater than the effective half-life T_e, which is the case for most radionuclides in tissue.

3.6 Multivariate chemometric techniques

Chemometric data analysis methods provide powerful tools for processing large data with various numerical techniques in order to extract useful information (Massart *et al.*, 1998). Chemometric techniques such as Principal Component Analysis (PCA) and Hierarchical Cluster Analysis (HCA) are applied in this study, to compute, to screen and to display graphical patterns in activity concentration and heavy metals elements, looking for possible groupings in terms of coltan type and sources of data variation.

3.6.1 Principle Component Analysis (PCA)

Principal component analysis (PCA) refers to a method used to transform and visualize complex multivariate measurements in low-dimensional spaces that are easier to interpret, without any significant loss of information. The linear multivariate PCA models are developed using orthogonal basis vectors (eigenvectors), which are usually called principal components. One of the significant goals of PCA is to eliminate the principal components associated with noise, thereby reducing the dimensionality of complex problems and minimizing the effects of measurement error. With PCA, It is possible to build an empirical mathematical model of data as described in the equation below where T_k is a $n \times k$ matrix of Principle Component scores and V_k is the $m \times k$ matrix of eigenvectors (Taylor, 2006).

33

$$A = T_k \ V_k^T + \varepsilon \qquad (3.23)$$

The eigenvectors in V_k can be used to form a set of orthonormal raw basis vectors for A. The eigenvectors are also called "loadings" or sometimes "abstract factors" or "eigenspectra" and ε is the residual part. The columns of T_k are called scores and are mutually orthogonal but not normalized. They can be used to form a set of column basis vector of A. For each independent source of variation in the data, a single PC (eigenvector) is expected in the model. The first PC explains as much as possible of the total variance of the data in matrix A. The second component explains as much as possible of the remaining variance and so on (Hedwig *et. al.*, 1990). Using PCA, activity concentrations of detected radionuclides and heavy metals more relevant to the quality of Rwandan Coltan may be identified.

3.7.2 Hierarchical Cluster Analysis (HCA)

The primary purpose of clustering techniques is to present the data in an approach that demonstrates the grouping in a multidimensional space in such a way that all objects in a single group have some natural relation to one another, and the objects from different groups are somewhat different from each other. The measurement of similarity between two objects or cluster is based mostly on the squared Euclidean distance. The Euclidian distance is defined as

$$d_{lk} = \sqrt{\sum_{j=1}^{J}\left(x_{kj} - x_{ij}\right)^2} \qquad (3.24)$$

where there are j measurements, and x_{ij} is the jth measurement of sample i= Euclidian distance coefficient between objects i and j. The Euclidian distance coefficient is calculated

for every pair of measurements. For example, with j number of measurements, $\frac{j(j-1)}{2}$ coefficients have to be calculated. Once the Euclidian distance coefficients have been measured, a similarity (or dissimilarity) matrix can be drawn up using Euclidian distance coefficient (Richard, 2007). Measurements are organized in a row, according to their similarities. Using nearest neighbour linkage and correlation coefficients for similarities, hierarchical clustering is represented in a graphical form called dendogram. In this study similarities in activity concentration of radionuclides and heavy metals were represented using HCA.

4.0 MATERIALS AND METHODS

4.1 Sampling and sample collection

Thirty-nine hand samples (processed coltan ore, extracted coltan ore, sediment, and soil) from various mines located in Muhanga (Southern province), Ruli (Northern province) and Ngoma (Eastern province) areas were collected, packed in polythene containers and labeled properly with sample identification number indicative of the mine location and the site (Figure: 4.1).
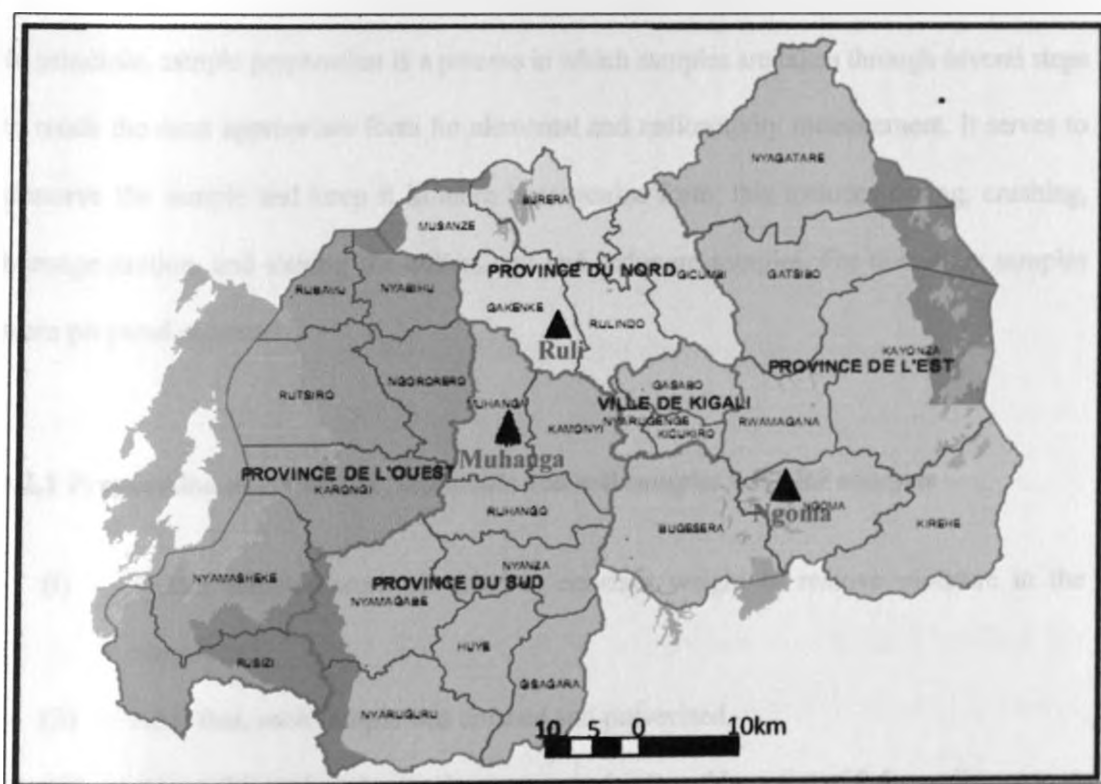
LEGENDE

☐ Limite de la province	▨ Lac		☐ PROVINCE DU NORD
☐ Limite de district	☐ PROVINCE DE L'EST	☐	☐ PROVINCE DU SUD
▬ Parcs	▬ PROVINCE DE L'OUEST	▬	VILLE DE KIGALI

Figure 4.1: Map of Rwanda indicating location of the three main coltan mining areas.

Each mining area was sub-divided into 5 sites in such a manner to represent the whole mining area and a control point was chosen outside the mining area. The control point is a reference point which helps to make a comparison between the levels of NORM in mining materials and in the local soil. At each of the areas, two processed coltan ore samples each weighing 0.5 kg, five extracted coltan ore samples each weighing 0.5 kg, five sediment samples weighing 0.5 kg, and one soil samples from a control point with respect to each region were also collected.

4.2 Samples preparation

In principle, sample preparation is a process in which samples are taken through several steps to reach the most appropriate form for elemental and radioactivity measurement. It serves to preserve the sample and keep it in more homogenize form; this includes drying, crushing, homogenization, and sieving the coltan, soil and sediment samples. For this study samples were prepared separately.

4.2.1 Preparation of coltan ore, sediments and soil samples for XRF analysis

(i)   Coltan samples were air dried to constant weight to remove moisture in the samples.

(ii)   After that, each sample was crushed and pulverized.

(iii)   About 0.5 g of each sample was pressed into a thin pellet of 2.5 cm diameter. A total of three pellets were made from each sample for replicate measurements.

(iv)   Each sample was irradiated for 2000 seconds live time and the spectral results recorded.

(v)   The same procedure was repeated for sediment and soil samples.

4.2.2 Preparation of coltan ore, sediments and soil samples for gamma-ray analysis

(i)   Coltan samples were dried to constant weight to remove moisture in the samples.

(ii)   After that, each sample was crushed and pulverized.

(iii)   About 300 g of each sample was sealed in 250 ml plastic beakers and stored for at least one month to allow the gaseous radon (half life 3.8 days) and its short decay daughters (^{214}Bi and ^{214}Pb) to achieve secular equilibrium with the long lived ^{226}Ra before gamma spectrometric analyses.

(iv)   The same procedure was repeated for sediment and soil samples.

4.3 Elemental analysis

Elemental analysis was performed using Energy Dispersive X-ray Fluorescence (EDXRF) system. The energy dispersive X-ray fluorescence analysis system consists of a Si(Li) detector, ^{109}Cd radioisotope excitation source and measurement electronics. The schematic diagram of an Energy Dispersive X-ray Fluorescence (EDXRF) spectrometer is shown in figure 4.2.

The radioactive source, ^{109}Cd (half life, $T_{1/2}$ = 453 days and activity = 10 mCi) irradiates the sample which then emits characteristic X-rays. These X-rays are detected by a Si(Li) detector (EG& G Ortec, 30 mm^2 x 10 mm sensitive volume, 25 μm Be window) with energy resolution of 195 eV at 5.9 KeV (Mn- K_α) line. A computer based MCA was used for Spectral data acquisition.
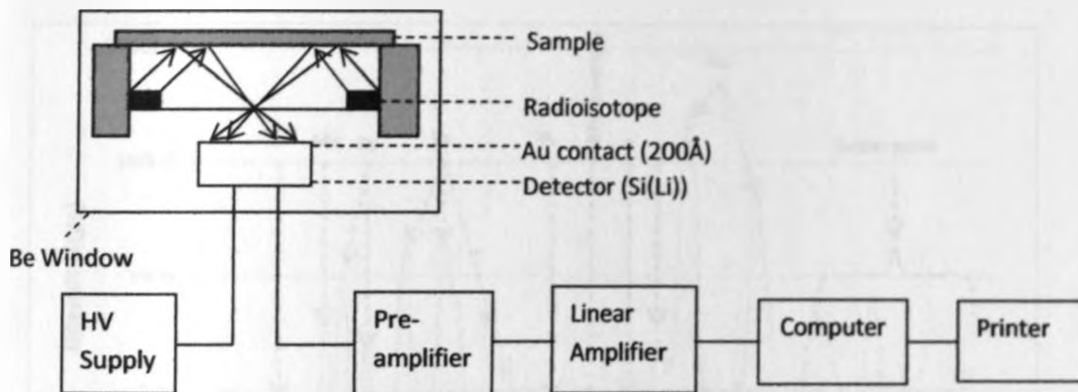
Figure 4.2: Block diagram of a radioisotope EDXRF spectrometer.

The characteristic X-ray spectra obtained from the samples were evaluated by non-linear least square fitting using the analysis of X-ray spectra by interactive least squares – quantitative X-ray analysis for thin samples (AXIL-QXAS) code (IAEA, 2005).

The QXAS (Quantitative X-ray Analysis System) software package is an integrated system for the quantitative evaluation of spectra measured with energy dispersive X-ray spectrometers. For the determination of the net peak intensities of characteristic lines of interest the AXIL (Analysis of X-ray spectra by Iterative least-squares fitting) is used.

Figures 4.3, 4.4., 4.5., and 4.6, show examples of typical EDXRF spectra obtained from samples of processed coltan, extracted coltan, sediment and soil from Muhanga area respectively.
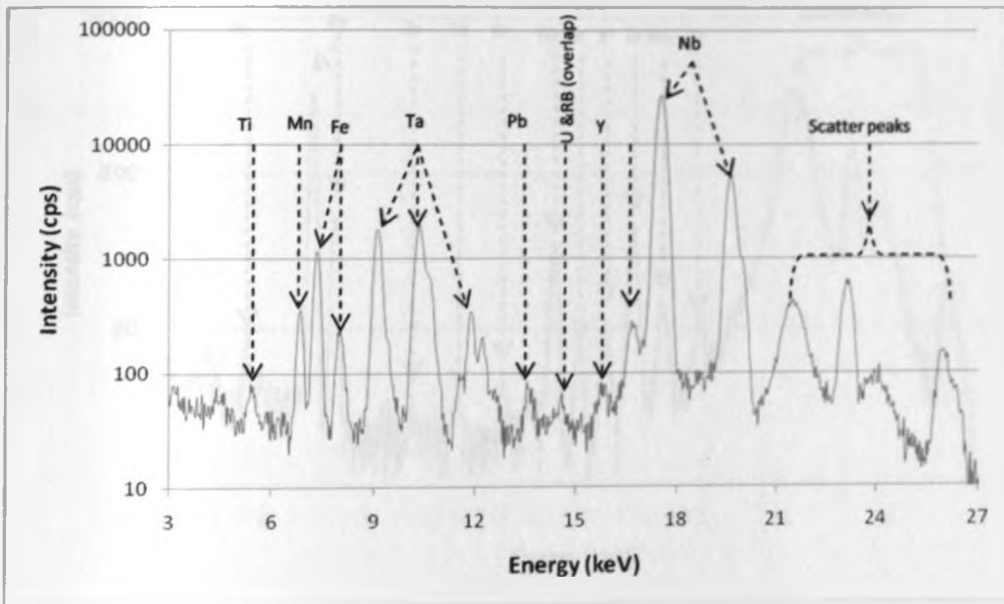
Figure 4.3: Typical EDXRF spectrum of processed coltan sample from Muhanga.
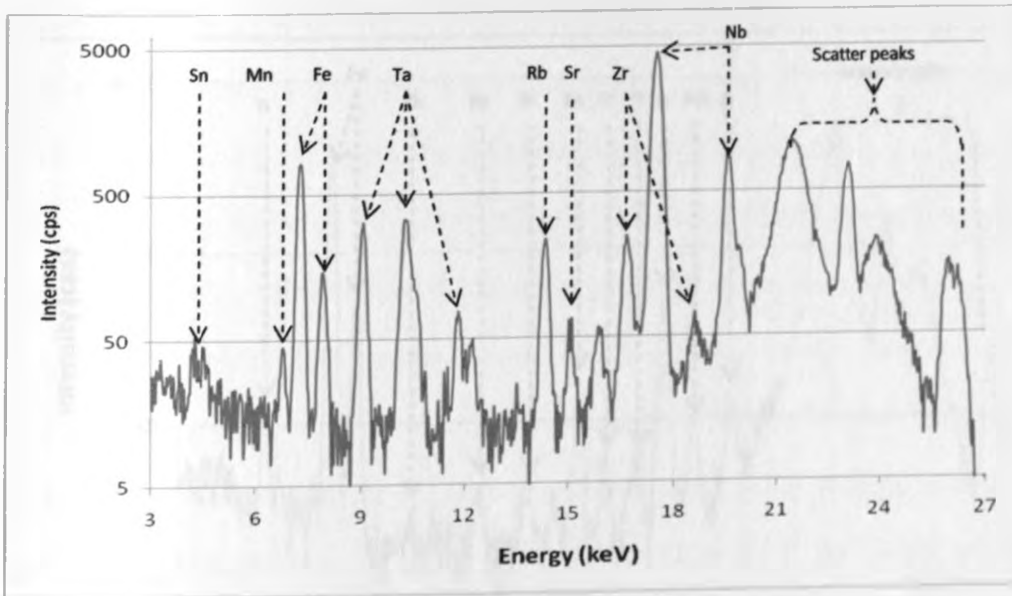
Figure 4.4: Typical EDXRF spectrum of extracted coltan sample from Muhanga.
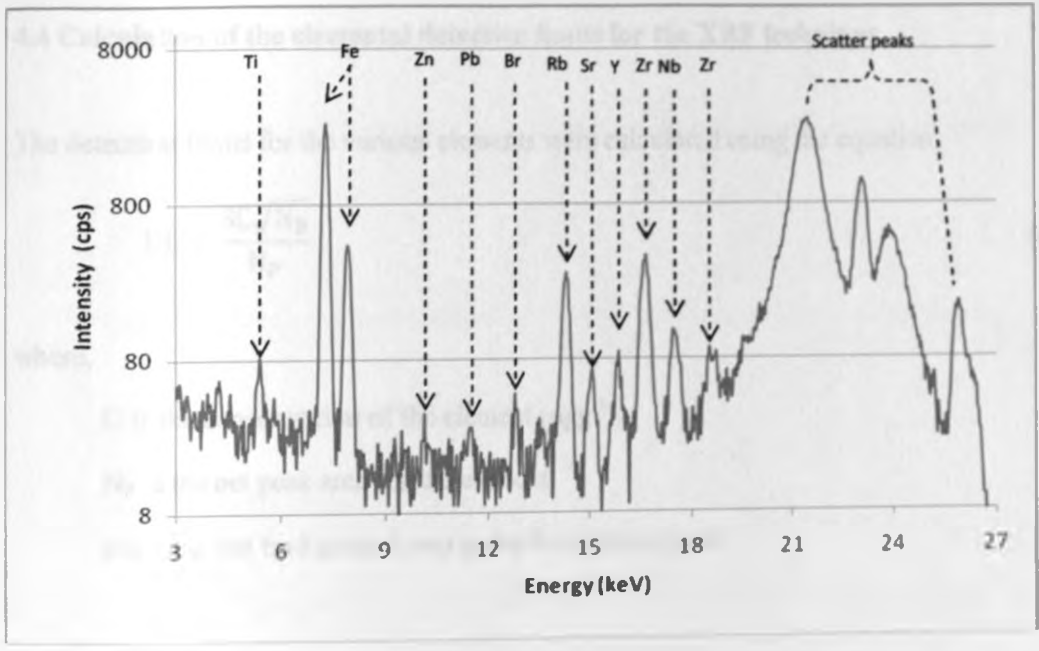
Figure 4.5: Typical EDXRF spectrum of sediment sample from Muhanga.
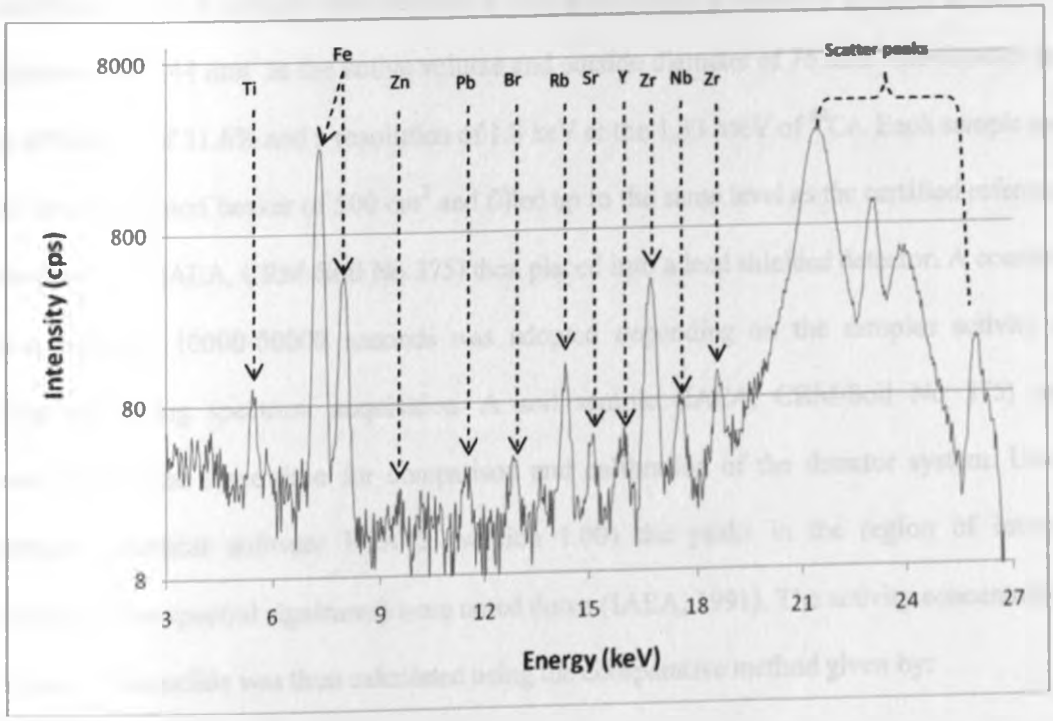
Figure 4.6: Typical EDXRF spectrum of soil sample from a control point from Muhanga.

41

4.4 Calculation of the elemental detection limits for the XRF technique

The detection limits for the various elements were calculated using the equation,

$$DL = \frac{3C\sqrt{N_B}}{N_P} \tag{4.1}$$

where,

C is the concentration of the element (μgg^{-1}).

N_P is the net peak area for the element.

N_B is the net background area under the element peak.

4.5 Gamma-ray spectrometric analysis

Measurement of activity concentrations of the naturally occurring radionuclides in coltan, sediments and soil samples was performed with high-purity germanium (HPGe) gamma-ray detector with 144 mm^3 as the active volume and outside diameter of 76 mm. The detector has an efficiency of 31.6% and a resolution of 1.8 keV at the 1.33 MeV of ^{60}Co. Each sample was put into a malineri beaker of 500 cm^3 and filled up to the same level as the certified reference standard soil (IAEA, CRM-Soil No 375) then placed into a lead shielded detector. A counting time between 10000-50000 seconds was adopted depending on the samples activity as observed during spectrum acquisition. A soil sample (IAEA, CRM-Soil No 375) was analysed for the same time for comparison and calibration of the detector system. Using gamma analytical software PCA 2 (version 1.00) the peaks in the region of interest (radionuclides spectral signitures) were noted down (IAEA, 1991). The activity concentration of each radionuclide was then calculated using the comparative method given by:

$$A_N = \frac{M_R A_R I_N}{M_S I_R} \tag{4.2}$$

where A_N is the activity of radionuclide N in the sample in Bq kg^{-1}.

M_R is the mass of reference soil sample in kg.

A_R is the activity of the parent radionuclide, in the reference sample from which N

belongs (Bq kg^{-1}).

I_N is the intensity of the radionuclide N in the soil sample in counts per second

obtained by fitting using GANAAS program.

M_s is the mass of the sample in kg.

I_R is the intensity of the radionuclide N in the reference soil in counts per seconds

obtained by fitting using GANAAS program.

The area under the spectral peaks was used to calculate the activity concentration in Bequerel

per kilogram (Bq kg^{-1}) in all samples. For each sample there were three significant gamma

lines; the ^{40}K line, ^{214}Pb line from ^{238}U and ^{212}Pb line from ^{232}Th. The activity of ^{40}K was

evaluated from the 1460 keV gamma line while the activity of ^{238}U from 351 keV gamma

line of ^{214}Pb and that of ^{232}Th from 238 keV gamma line of ^{212}Pb.

4.6 Detection limits of the gamma-ray analysis

The lower detection limits (LDL) for the various radionuclides were calculated using the

equation,

$$DL = \frac{3}{m}\sqrt{\frac{R_b}{T_b}} \tag{4.3}$$

where,

R_b is the background counts,

T_b is the background time, and

m is the sensitivity of the detector in Cs^{-1} per µg.

4.7 Methods used for estimating radiation dose exposures

Two methods of evaluating external exposure from naturally occurring radionuclides have been used. The first is simply to summarize directly measured external gamma dose rates in air. The second is to calculate the external gamma dose rates in air from measurements of the concentrations of the relevant radionuclides in samples.

4.7.1 Measurement of absorbed dose rates in air

Dose rates (cps) at 1m above the ground were measured using an appropriately calibrated Sensor Meter, Model G/B. Absorbed dose rates in air in nGyh⁻¹ were computed from the dose rates in µSv h⁻¹ as measured in the field using the conversion coefficient factor of 0.7Sv Gy⁻¹ as recommended by UNSCEAR (2000).

4.7.2 Calculation of absorbed dose from measured activity concentrations

The main routes of exposure to artisans mining coltan ore depend on different working scenarios during the mining operations. These include the external exposure from gamma radiation in the ground containing coltan ore, internal exposure from inhalation of coltan dust in the air, internal exposure from inadvertent ingestion of coltan, and external exposure from submersion in air contaminated with coltan dust. The radiation doses that are likely to accrue from each working or exposure scenario were calculated using existing generic models that

closely describe exposure scenarios. Typical input parameters include the activity concentrations of the relevant radionuclides in various types of materials, working habit data (e.g. exposure duration, breathing rates, etc.) and the dose coefficients. Other parameters, including dose coefficients, were adopted from the literature (Ekerman and Ryman, 1993; ICRP, 1994). Descriptions of the models used for calculating doses from each exposure pathway are presented in the following section.

(i) External Dose due to irradiation by γ-rays from radionuclides in the ground

External sources of radiation exposure to mine workers are caused by the concentration of naturally occurring radioactive materials present in the deposited mineral (UNSCEAR, 1993). The absorbed gamma dose rates in air at 1 m above the ground surface for the uniform distribution of radionuclides are computed on the basis of guidelines provided by UNSCEAR (1993, 2000).

$$D = 0.666\, A_{Th} + 0.042\, A_k + 0.429\, A_{Ra} \tag{4.4}$$

where D represents total absorbed dose in air nGy h^{-1}. A_{Th}, A_K and A_{Ra} are the activity concentrations of ^{232}Th, ^{40}K and ^{226}Ra respectively, present in the ore and sediment samples. The contents on the right hand side of the equation (4.4) are related to the average gamma-ray energies for each radionuclide or series. Dose conversion factor or dose coefficient represent the dose rate in air per unit activity concentration of radionuclides in the soil sample and is expressed in nGy h^{-1} per Bq kg^{-1} (Tahir *et al.*, 2005). The relationship was based on the dose conversion factors recommended by the UNSCEAR (1993), for the estimation of the total air absorbed outdoor gamma radiation. It is noted that the calculation of these DCFs has been based on the assumption that the decay products of the ^{226}Ra and ^{232}Th series are in the radioactive equilibrium with their precursors (Sam and Elmahadi, 2007).

The external effective dose D_{ext} (Sv y^{-1}) received by an individual due to the distribution of coltan in the immediate environment can be calculated using equation

$$D_{ext} = \sum_R A_R DC_{ext,R} CF_s T \tag{4.5}$$

where A_R is the activity concentration of gamma-ray emitting radionuclides in coltan (Bq g^{-1}) and $DC_{ext,R}$ is the effective dose coefficient for the radionuclide R in nSv h^{-1} per Bq g^{-1}. For digging, external exposure the value of $DC_{ext,R}$ were obtained from UNSCEAR (2000) report i.e 350 (nSv h^{-1} per Bqg^{-1}) for ^{238}U series, 510 (nSv h^{-1} per Bq g^{-1}) for ^{232}Th series and 33 (nSv h^{-1} per Bq g^{-1}) for ^{40}K series. Table 4.1 gives the values of $DC_{ext,R}$ for the rest of the working scenarios; CF_s is the enhancement factor between coltan and other environmental materials, CF_s are 10^{-3} for coltan-bearing soil, mine dust, and slurry and 1 for mill dust and all grades of coltan (wet, dry, coarse, fine, etc) (Mustapha et al., 2007), and T is the exposure time in hours.

Table 4.1: Effective dose coefficients for external exposure to radionuclides including contributions of short lived daughters (Eckerman and Ryman (1993)).

Radionuclides	Effective dose coefficients (nSv h^{-1} per Bq g^{-1})				Air submersion (nSv h^{-1} per Bq m^{-3})
	Soil contaminated to			Contaminated surface	
	1 cm	5 cm	Infinite depth		
^{40}K	5.472	15.552	30.701	1.175	0.029
^{226}Ra	60.224	172.975	327.514	9.929	0.302
^{228}Ra	33.178	95.040	175.528	5.409	0.162
^{228}Th	51.553	148.951	298.616	8.299	0.276
^{230}Th	0.012	0.027	0.033	0.004	0
^{232}Th	0.006	0.012	0.014	0.003	0
^{234}U	0.005	0.009	0.011	0.003	0
^{238}U	1.205	2.467	3.700	0.688	0.005

(ii) Internal dose due to inhalation of air contaminated with dust

The effective dose due to inhalation of contaminated air with dust D_{inh} (Sv y^{-1}) was then calculated using the equation:

$$D_{inh} = \sum_R A_R DC_{inh,R} C_d I_w T \qquad (4.6)$$

where $DC_{inh,R}$ is the effective dose coefficient for radionuclide R (nSv Bq^{-1}), the values of $DC_{inh,R}$, C_d is the total dust loading (g m^{-3}), I_w is the inhalation rate, and T and A_R have been defined in equation (4.3). In this study, the rationale applied in determining suitable dust loading were based on a similar one presented by Oatway and Mobbs (2003). According to Oatway and Mobbs (2003), the dust load value (in g m^{-3}) used are 10^{-3} for manual digging and handling coltan in open mine, 10^{-2} for crushing and sieving coltan in the mills, and 5×10^{-3} for drying coltan. The inhalation rates ($m^3 h^{-1}$) are 1.2 for drying coltan and 1.69 for the rest of the scenarios. Table 4.2 shows the values of $DC_{inh,R}$ obtained from ICRP 68 (ICRP, 1994).

Table 4.2: Effective dose per unit intake of selected radionuclides including contributions of short-lived daughters (ICRP (1994)). (Moderate (M) and slow (S) absorption rates were selected for insoluble ores).

Radionuclides	Committed effective dose per unit intake (nSv Bq^{-1})	
	By inhalation (Absorption type)	By ingestion (Fractional adsorption)
^{226}Ra	5600 (M)	1200 (0.2)
^{228}Ra	1700 (M)	670 (0.2)
^{228}Th	34500 (S)	106 (0.0002)
^{230}Th	7200 (S)	87 (0.0002)
^{232}Th	12000 (S)	92 (0.0002)
^{234}U	6800 (S)	8 (0.002)
^{238}U	5700 (S)	12 (0.002)

(iii) Internal dose due to inadvertent ingestion of radionuclides

The effective dose D_{ing} (Sv y^{-1}) due to inadvertent ingestion of radionuclides was calculated using the equation

$$D_{ing} = \sum_R A_R DC_{ing,R} I_{ing,R} T \tag{4.7}$$

where $DC_{ing,R}$ is the effective dose coefficient for ingestion (Sv Bq^{-1}) (Table 4.2), $I_{w,ing}$ is the ingestion rate and all other terms have same meaning as described earlier. Inadvertent ingestion is assumed to occur through hand to mouth transfer of contaminated soil and dust present on the skin and clothing. For the purposes of this research the amount of soil that is likely to be inadvertently ingested by an adult in these working conditions is assumed to be 5×10^{-3} g h^{-1} (Oatway and Mobbs, 2003). The T was taken to be 2500 hours in a year for a miner working for eight hours for six days in a week for 52 weeks for the digging, crushing and panning scenarios.

(iv) External exposure due to submersion in contaminated air

This kind of exposure occurs when artisans work in an environment that contains suspended radionuclides, e.g when digging, grinding or milling coltan. The effective dose due to submersion D_{subm} (nSv y^{-1}) is calculated using the following formula:

$$D_{Subm} = \sum_R A_R CF_d DC_{subm,R} C_d T \tag{4.8}$$

where D_{subm} is the effective dose from submersion in contaminated, A_R is the activity concentration R (Bq g^{-1}) in coltan, CF_d is the fraction of coltan in the suspended matrix (soil dust), $DC_{subm,R}$ is the effective dose-conversion coefficient for submersion in contaminated air for radionuclide R (nSv h^{-1} per Bq m^{-3}), C_d is the concentration of dust in air, 10^{-2} g m^3 (Oatway and Mobbs, 2003), T is the occupancy time, assumed to be 2500 h y^{-1}. $DC_{subm,R}$ are

2.898x10^{-2} (nSv h^{-1} per Bq m^{-3}), 1.2276x10^{-5} (nSv h^{-1} per Bq m^{-3}) and 3.1392x10^{-5} (nSv h^{-1} per Bq m^{-3}) for ^{40}K, ^{238}U and ^{232}Th respectively.

(v) The total effective dose for each exposure scenario

The total annual effective dose, D_{Tot}, received by the artisans who dig and/or handle ores and slurries containing coltan is the sum of the doses from external irradiation by gamma-rays emitted by radionuclides contained in the ground and the environment, submersion in air containing dust, inhalation of air contaminated by dust and inadvertent ingestion of radionuclides in dust. This is given by the equation

$$D_{Tot} = D_{ext} + D_{ing} + D_{inh} + D_{subm} \tag{4.9}$$

Chapter 5

5.0 RESULTS OF ANALYSIS AND DISCUSSION

5.1 Elemental concentrations

5.1.1 Accuracy of the EDXRF Analysis method

The quality assurance of the method was carried out on standard certified reference materials

i.e soil-7 and thick samples (Tantalum (Ta), Niobium (Nb), Tin (Sn)) produced by IAEA. The

results obtained were compared with the certified reference values from the IAEA-certificate

as shown in Table 5.1 and Table 5.2 below.

Table 5.1: Results of EDXRF analysis of IAEA certified reference material soil-7.

Element	Experimental values ($\mu g\ g^{-1}$ or %)	Certified values ($\mu g\ g^{-1}$ or %)	Confidence interval ($\mu g\ g^{-1}$ or %)
K	10800	12100	11300 -12700
Ca	16.8%	16.3%	(15.7 - 17.4) %
Ti	3650	3000	2600 – 3700
Mn	636	631	604 – 650
Fe	2.7%	2.57%	(2.52 – 2.63) %
Zn	103	104	101 – 113
Pb	50.7	76	55 – 71
Br	6.5	7	3 – 10
Rb	48.7	51	47 – 46
Sr	102	108	103 – 114
Y	19.5	21	15 – 27
Zr	188	185	180 – 201
Nb	9.9	12	7 – 17

Table 5.2: Result of EDXR analysis of IAEA certified thick samples (Ta, Nb, Sn)

Element	Experimental values (%)	Certified value (%)
Ta	105	99.999
Nb	107	99.999
Sn	97.8	99.999

From Table 5.1 and Table 5.2, most of the concentration values agree with the certified concentration values. This, therefore, demonstrates the reliability and accuracy of the method i.e. Energy-Dispersive X-Ray Fluorescence (EDXRF) analysis.

5.1.2 Elemental fluxes of coltan ores, sediments and soils

Energy Dispersive X-Ray Fluorescence (EDXRF) analysis was used to identify and quantify heavy elements in coltan ores, sediments and soil samples. The detected heavy elements can be classified into 3 groups i.e coltan-dependent elements (Ta, Nb, Sn), heavy toxic elements (Pb, Mn, Zn) and radioactive elements (U, Th, Sr, Pb, Rb). The results are presented in Tables 5.3 to 5.5 and in Figures 5.1 to 5.5.

Table 5.3: Average elemental fluxes (mg g^{-1}) of samples from Muhanga area.

EL	Processed coltan ore (n=2) $\bar{X}\pm1SD$	Range (Min-Max)	Extracted coltan ore (n=5) $\bar{X}\pm1SD$	Range (Min-Max)	Sediment (n=5) $\bar{X}\pm1SD$	Range (Min-Max)	control point soil (n=1)
K	33.1 ± 4.5	(32.2 - 33.9)	14.5 ± 2.4	(3.43 - 30.05)	11.2 ± 1.2	(4.34 - 17.9)	8.56 ± 0.33
Sn	161 ± 5	(158 - 164)	<4.4	<4.4	<4.4	<4.4	<4.4
Ti	30.3 ± 0.9	(28.7 - 31.8)	0.810 ± 0.140	(0.125 - 1.96)	2.46 ± 0.37	(0.575 - 4.51)	5.65 ± 0.33
Mn	65.2 ± 0.4	(64.8 - 65.6)	7.40 ± 0.89	(1.52 - 26.9)	<0.104	(0.043 - 0.116)	0.201 ± 0.024
Fe	167 ± 1	(166 - 168)	54.8 ± 7.6	(25.5 - 121)	21.2 ± 2.0	(8.27 - 32.6)	38.7 ± 0.8
Zn	2.20 ± 0.03	(2.00 - 2.40)	0.168 ± 0.035	(0.019 - 0.463)	0.023 ± 0.004	(0.004 - 0.058)	0.034 ± 0.003
Ta	228 ± 2	(225 - 232)	29.3 ± 6	(8.63 - 81.5)	0.035 ± 0.005	(0.019 - 0.080)	<0.031
Ga	<0.021	<0.021	0.120 ± 0.020	(0.057 - 0.305)	0.048 ± 0.004	(0.016 - 0.068)	<0.021
Pb	3.65 ± 0.10	(3.30 - 4.02)	0.960 ± 0.066	(0.088 - 4.24)	0.044 ± 0.002	(0.035 - 0.065)	0.041 ± 0.002
Rb	0.180 ± 0.050	(0.172 - 0.189)	0.330 ± 0.045	(0.102 - 0.603)	0.321 ± 0.040	(0.185 - 0.676)	0.105 ± 0.005
Sr	0.113 ± 0.001	(0.110 - 0.115)	0.050 ± 0.004	(0.034 - 0.091)	0.038 ± 0.003	(0.019 - 0.052)	0.035 ± 0.004
Th	0.577 ± 0.035	(0.569 - 0.585)	0.079 ± 0.010	(0.039 - 0.174)	0.011 ± 0.001	(0.006 - 0.016)	0.011 ± 0.001
U	4.35 ± 0.02	(0.725 - 7.97)	0.071 ± 0.01	(0.019 - 0.198)	<0.007	<0.007	<0.007
Zr	1.86 ± 0.02	(1.82 - 1.91)	0.470 ± 0.044	(0.273 - 0.832)	0.149 ± 0.002	(0.053 - 0.257)	0.300 ± 0.001
Nb	256 ± 3	(256 - 257)	27.1 ± 6.6	(6.75 - 85.6)	0.055 ± 0.008	(0.024 - 0.120)	0.040 ± 0.001

n= number of samples, $\bar{X}$ = Average, SD= Standard deviation, Min= Minimum, Max= Maximum, EL= Element

Table 5.4: Average elemental fluxes (mg g^{-1}) of samples from Ruli area.

EL	Processed coltan ore (n=2)		Extracted coltan ore (n=5)		Sediment (n-=5)		control point (soil) (n=1)
	$\bar{X}\pm1SD$	Range (Min-Max)	$\bar{X}\pm1SD$	Range (Min-Max)	$\bar{X}\pm1SD$	Range (Min-Max)	
K	17.3 ± 0.8	(15.8 - 18.8)	19.7 ± 1.8	(9.606 – 30.875)	17.3 ± 0.880	(11.79 – 23.06)	22.3 ± 0.3
Sn	91.9 ± 2.7	(89.4 – 94.5)	< 4.4	< 4.4	< 4.4	< 4.4	< 4.4
Ti	18.7 ± 0.1	(18.6 – 18.7)	3.9 ± 0.7	(0.428 – 8.36)	3.90 ± 0.30	(1.80 – 5.60)	5.40 ± 0.21
Mn	35.2 ± 4.9	(21.3 – 49.0	1.78 ± 0.36	(0.240 – 4.73)	0.270 ± 0.046	(0.056 – 0.640)	< 0.104
Fe	144 ± 1	(135 – 153)	16.3 ± 0.5	(5.98 – 25.5)	32.65 ± 1.60	(20.50 – 40.19)	43.2 ± 1.4
Zn	21.0 ± 2.8	(15.8 – 26.2)	0.132 ± 0.007	(0.061 – 0.204)	0.043 ± 0.006	(0.024 - 0.074)	0.019 ± 0.003
Ta	225 ± 3	(223-228)	3.18 ± 0.40	(0.988 – 6.337)	0.040 ± 0.007	(0.019 – 0.101)	< 0.032
Ga	< 0.021	< 0.021	0.038 ± 0.005	(0.018 – 0.086)	0.026 ± 0.002	(0.015 – 0.037)	< 0.021
Pb	0.550 ± 0.014	(0.543 – 0.553)	0.097 ± 0.003	(0.069 – 0.114)	0.068 ± 0.006	(0.041 – 0.111)	0.049 ± 0.002
Rb	0.182 ± 0.005	(0.170 – 0.194)	1.80 ± 0.11	(1.13 – 2.37)	0.590 ± 0.067	(0.137 – 1.04)	0.980 ± 0.020
Sr	0.054 ± 0.003	(0.053 – 0.056)	0.280 ± 0.003	(0.088 – 0.476)	0.160 ± 0.020	(0.064 – 0.319)	0.123 ± 0.001
Th	0.295 ± 0.005	(0.274 – 0.317)	0.032 ± 0.002	(0.017 – 0.460)	0.015 ± 0.001	(0.008 – 0.018)	0.0117 ± 0.001
U	0.307 ± 0.020	(0.281 – 0.334)	0.013 ± 0.001	(0.007 – 0.031)	0.004 ± 0.0004	(0.002 – 0.006)	0.008 ± 0.001
Zr	1.72 ± 0.08	(1.672 – 1.768)	0.299 ± 0.036	(0.066 – 0.486)	0.199 ± 0.003	(0.009 – 0.335)	0.236 ± 0.007
Nb	162 ± 5	(156 – 167)	2.07 ± 0.24	(0.434 – 3.61)	0.033 ± 0.003	(0.004 – 0.056)	0.490 ± 0.029

n= number of samples, $\bar{X}$ = Average, SD= Standard deviation, Min= Minimum, Max= Maximum, EL= Element

Table 5.5: Average elemental fluxes (mg g^{-1}) of samples from Ngoma area.

EL	Processed coltan ore (n=2)		Extracted coltan ore (n=5)		Sediment (n=5)		Control point (Soil) (n=1)
	$\bar{X}\pm 1SD$	Range (Min-Max)	$\bar{X}\pm 1SD$	Range (Min-Max)	$\bar{X}\pm 1SD$	Range (Min-Max)	
K	33.8 ± 2.9	(30.7 – 37.0)	20.9 ± 1.6	(13.6 – 33.7)	13.2 ± 1.5	(2.11 – 22.1)	8.58 ± 0.10
Sn	77.5 ± 6.7	(74.5 – 80.5)	< 4.4	< 4.4	<4.4	<4.4	<4.4
Ti	1.14 ± 0.13	(1.08 – 1.20)	3.03 ± 0.46	(0.931 – 7.01)	3.80 ± 0.43	(0.420 – 5.572)	7.70 ± 0.21
Mn	86.4 ± 0.28	(84-1 – 88.7)	5.24 ± 0.68	(0.811 – 9.44)	0.117 ± 0.012	(0.106 – 0.183)	0.970 ± 0.022
Fe	118 ± 1	(117 - 121)	46.5 ±3.4	(31.7 – 73.9)	35.7 ± 2.5	(13.62 – 43.37)	84.7 ± 0.7
Zn	1.18 ± 0.03	(1.14 – 1.22)	0.110 ± 0.001	(0.026 – 0.195)	0.042 ± 0.002	(0.025 – 0.056)	0.125 ± 0.016
Ta	304 ± 4	(303 - 306)	34.5 ± 3.6	(6.7 – 51.0)	0.084 ± 0.009	(0.032 – 0.146)	<0.032
Ga	< 0.021	< 0.021	0.120 ± 0.008	(0.062 – 0.164)	< 0.021	< 0.021	<0.021
Pb	0.717 ± 0.010	(0.695 – 0.740)	0.229 ± 0.013	(0.119 – 0.290)	0.113 ± 0.008	(0.048 – 0.160)	0.041 ± 0.004
Rb	0.188 ± 0.006	(0.185 – 0.191)	0.170 ± 0.016	(0.100 – 0.307)	0.265 ± 0.004	(0.246 – 0.299)	0.062 ± 0.002
Sr	0.050 ± 0.005	(0.047 – 0.053)	0.051 ± 0.005	(0.021 – 0.084)	0.073 ± 0.004	(0.037 – 0.094)	0.095 ± 0.004
Th	0.319 ± 0.006	(0.316 – 0.323)	0.063 ± 0.008	(0.017 – 0.107)	0.015 ± 0.001	(0.006 – 0.021)	0.091 ± 0.003
U	0.345 ± 0.037	(0.340 – 0.351)	0.071 ± 0.009	(0.0480 – 0.122)	< 0.007	< 0.007	<0.007
Zr	1.06 ± 0.03	(1.052 – 1.070)	0.498 ± 0.039	(0.280 – 0.686)	0.177 ± 0.016	(0.039 – 0.238)	0.382 ± 0.009
Nb	235 ± 3	(233 - 238)	20.4 ± 3.1	(9.71 – 37.3)	0.063 ± 0.007	(0.021 – 0.118)	0.108 ± 0.006

n= number of samples, $\bar{X}$ = Average, SD= Standard deviation, Min= Minimum, Max= Maximum, EL= Element
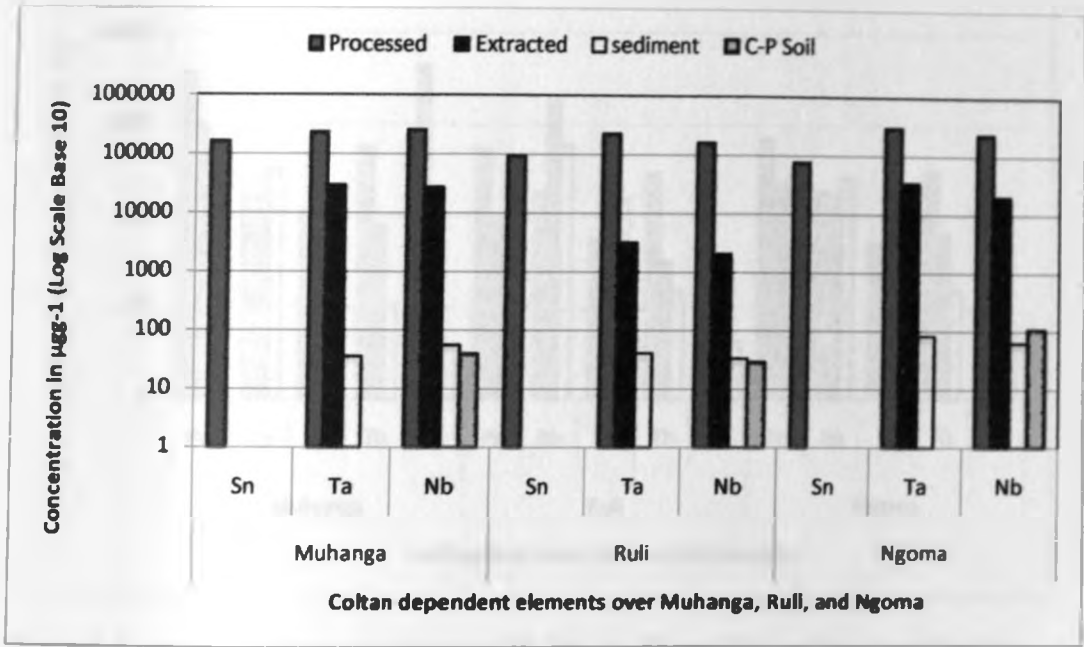
Figure 5.1: Level of coltan dependent elements (Sn, Ta and Nb) in samples from Muhanga, Ruli and Ngoma.
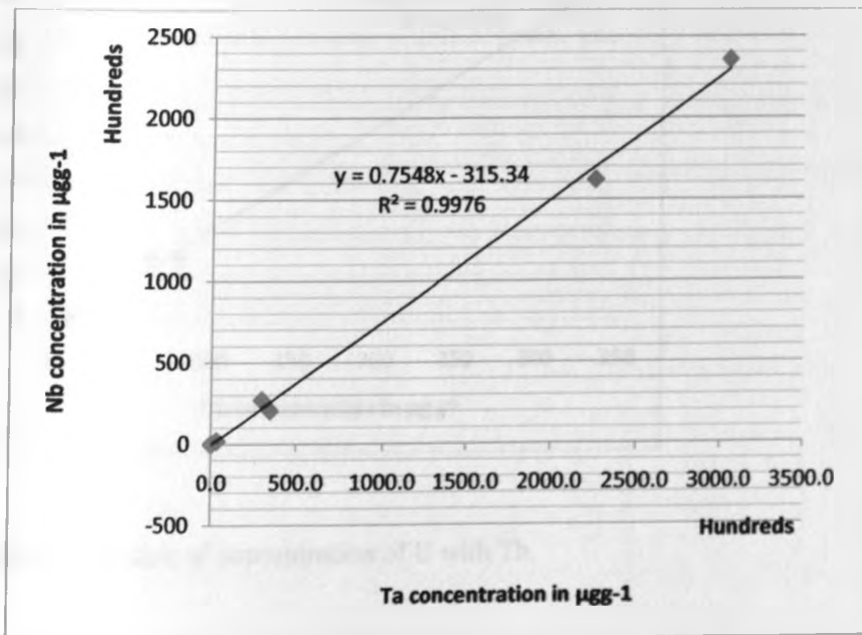

Figure 5.2: Correlation of concentration of Ta with Nb.
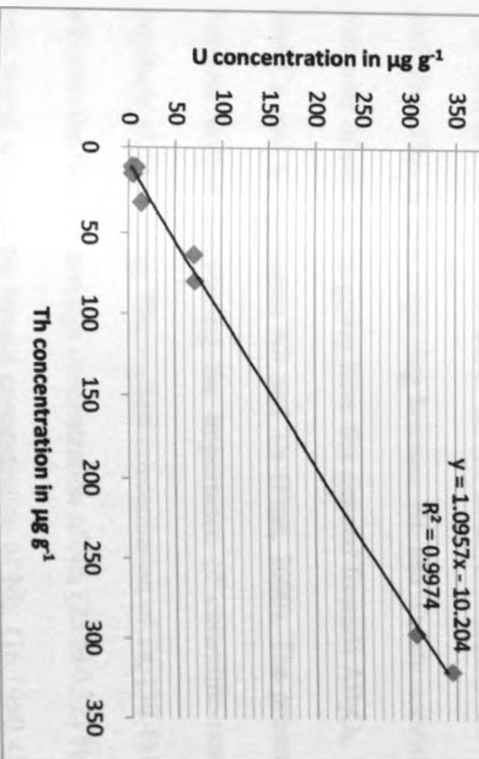
Figure 5.4: Correlation of concentration of U with Th.

56
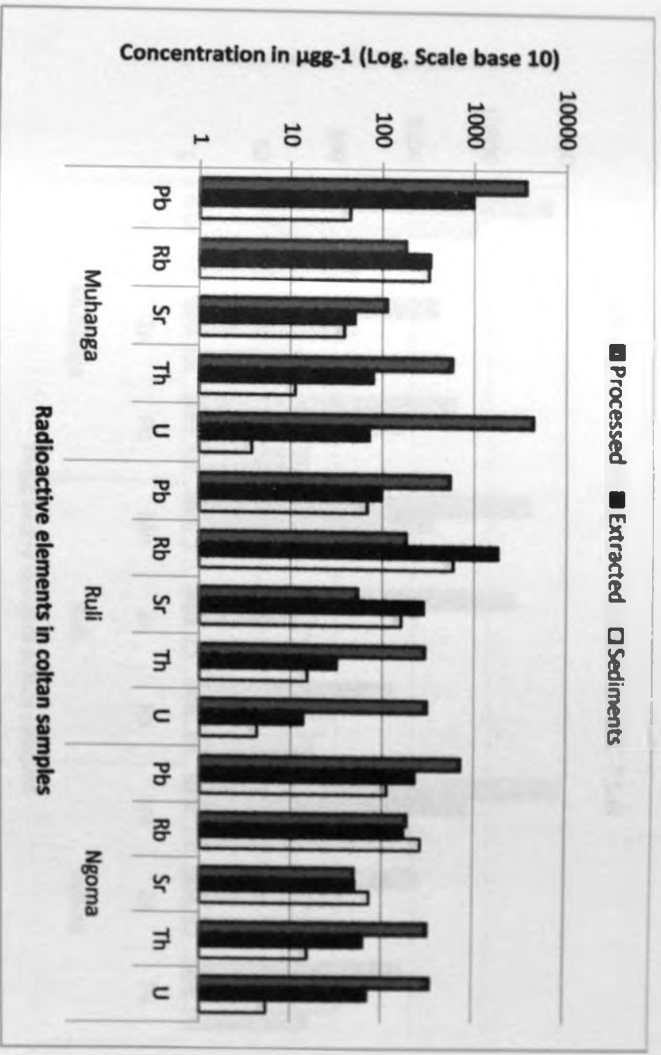
Figure 5.3: Level of radioactive elements (Pb, Rb, Sr, Th and U) in coltan samples from Muhanga, Ruli and Ngoma.
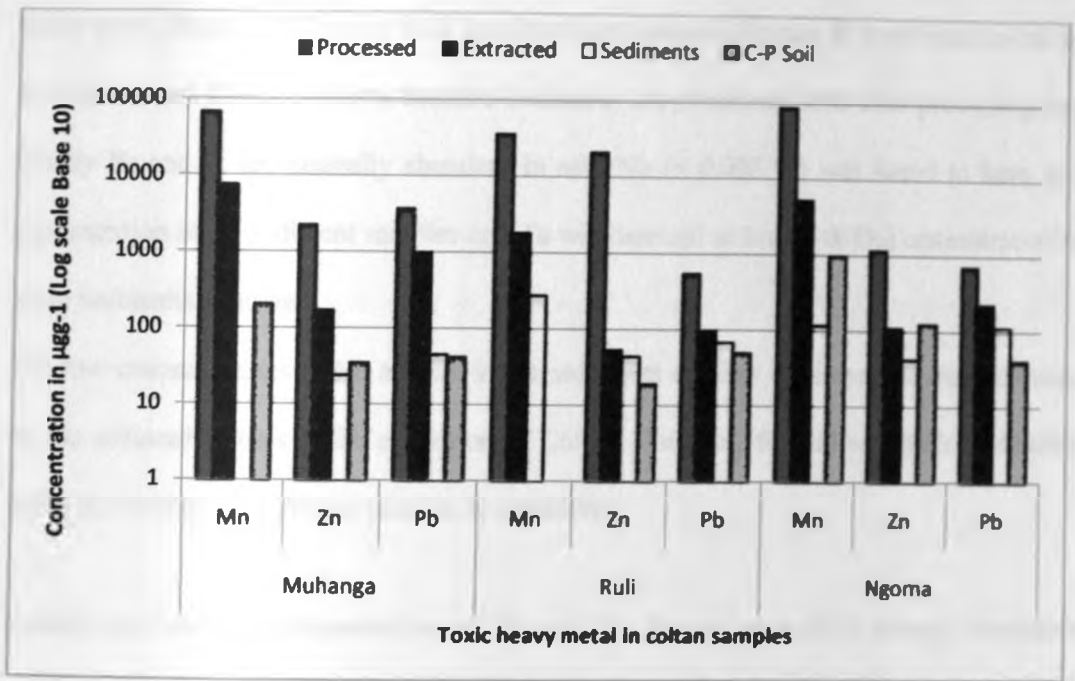
Figure 5.5: Level of heavy toxic elements in coltan samples from Muhanga, Ruli and Ngoma.

Ta, Nb, and Sn were found to be the most abundant in the tested columbite-tantalite ore samples. This is not surprising because Nb and Ta are normally extracted from coltan and minerals of columbite-group have the general formula AB_2O_6, where A represents Fe^{2+}, Mn and Ca and B represents Nb and Ta (Fuat, 2000). The presence of Sn was also expected because before discovering the importance of columbite-tantalite, Ta and Nb were by-products of Sn mining. The highest concentration of Ta, (30.4±0.45) % was found in Ngoma whereas the highest average concentration of Nb, (25.6±0.32) % was found in Muhanga. Ruli was found to have the lowest concentration of Nb, (16.19±0.48) % and Ta, (22.5±0.35) %. The average concentrations of Sn in all processed coltan were (16.1±0.47) %, (9.19±0.27) % and (7.75±0.67) % for Muhanga, Ruli and Ngoma areas respectively. Sn was found below the detection limit (0.44 %) in all areas for extracted, sediments and soil samples. This means that the concentration of Sn increase after processing coltan. The results of elemental analysis of all extracted coltan showed that Muhanga area has the highest concentration of Ta and Nb

followed by Ngoma and finally Ruli. In all sediment samples Fe and K were found to be the most abundant. This is obvious because sediments are remaining soils after processing and usually Fe and K are naturally abundant in soil. Nb (< 0.006 %) was found to have low concentration in all sediment samples and Ta was detected at low (0.008%) concentration in some sediments samples.

The low concentrations of Nb and Ta in the sediments confirm the improved methods used by the artisanal miners in the extraction of Coltan. However, for full economic realization better processing technologies need to be considered.

Comparison between concentration of Ta and Nb showed a positive strong correlation coefficient (0.95) between concentration of Tantalum (Ta) and Niobium (Nb) in all the three areas. This means that knowing the amount of one element one can predict the concentration of the other element for the same area under consideration (Figure: 5.2).

Heavy toxic elements such as Pb, Mn and Zn were also found in all mines. Mn was found to have the highest concentration (~6 %) whereas Zn was found to have the lowest concentration in all the samples (0.024 mg g^{-1}). Toxic elements can enter the human body by inhalation or ingestion, leading to many health risks. At high level of exposure, lead can severely damage the brain and kidneys in adults or children and ultimately cause death. In expectant women, high levels of exposure to lead may cause miscarriage and in men it can damage the organs responsible for sperm production (Nriagu, 1998). These elements are also said to be initiators or promoters of carcinogenic activities in animals (Nriagu, 1998).

To reduce exposure to toxic elements, the miners may need to take precaution by using the correct protective gears and observe personal hygiene practices such as washing hands

especially before meals. The government should also enforce and ensure that mining regulations on health and safety are adhered to by all miners.

Radioactive elements such as U, Th, Rb, Sr and Pb were found in some samples. Th, U and K were found in high concentration in all processed Coltan. Their average concentrations were (0.115-0.57) mg g^{-1}, (0.28-0.79) mg g^{-1} and (15.87-37.9) mg g^{-1} respectively. In most sediments samples these elements were below the detection limits. This shows that most of the radioactivity comes from processed coltan.

Comparison of Uranium (U) and Thorium (Th) also showed a positive correlation (0.99). This means that knowing the amount of one element we can predict the concentration of the other element (Figure: 5.2).

5.2 Activity concentration of natural radionuclides in coltan ores, sediments and soils

Radioactivity concentrations of ^{238}U, ^{232}Th and ^{40}K in coltan ores, sediments and soil samples were measured by gamma-ray spectrometry. The activity concentrations of ^{232}Th and ^{238}U were calculated from the gamma photo-peaks of ^{212}Pb (238 keV) and ^{214}Pb (351 keV) for thorium and uranium respectively while that of ^{40}K was evaluated from the 1460 keV gamma line. Figures 5.6, 5.7., 5.8., and 5.9, show examples of typical HPGe gamma spectra for samples of processed coltan, extracted coltan, sediment and soil from Muhanga area.
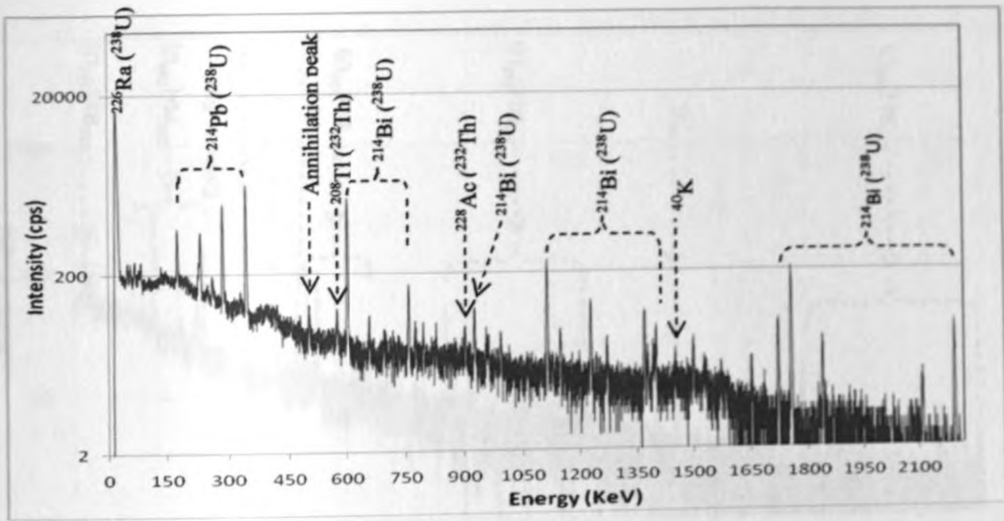
Figure 5.6: Typical gamma-ray spectrum of processed coltan sample from Muhanga.
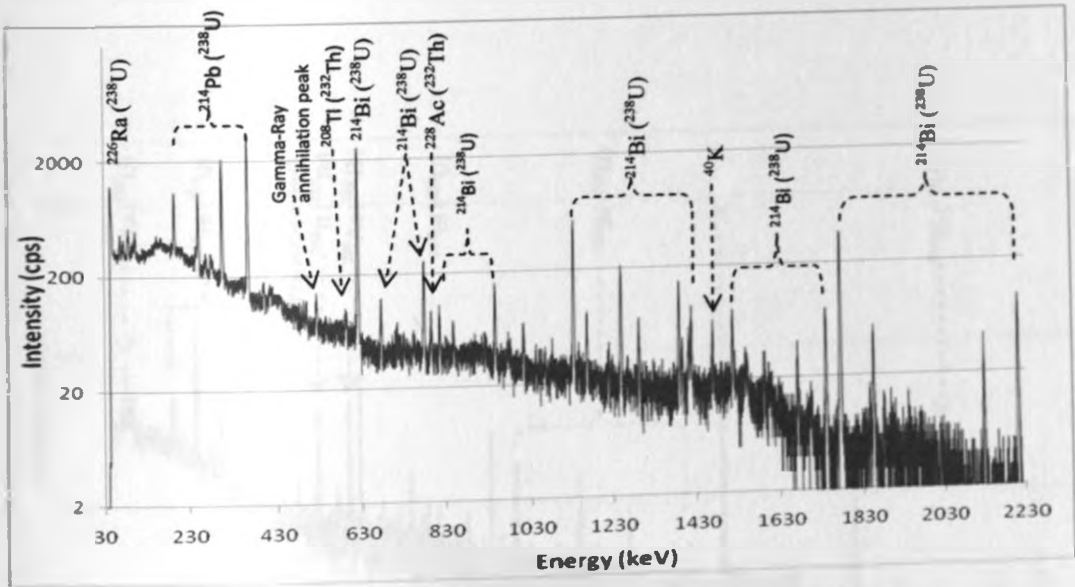
Figure 5.7: Typical gamma-ray spectrum of extracted coltan sample from Muhanga.
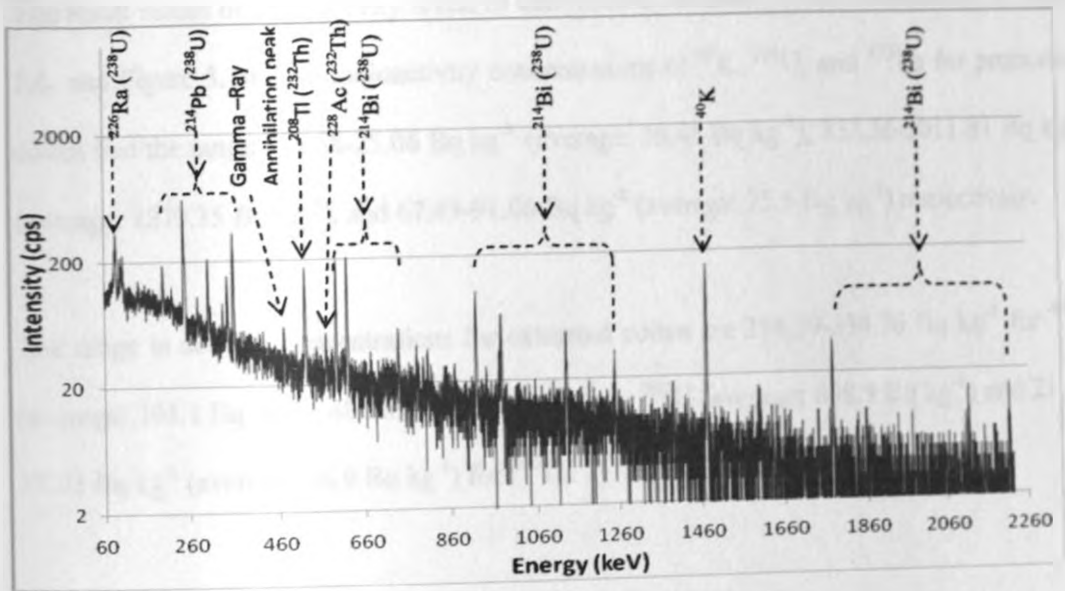
Figure 5.8: Typical gamma-ray spectrum of sediment sample from Muhanga.
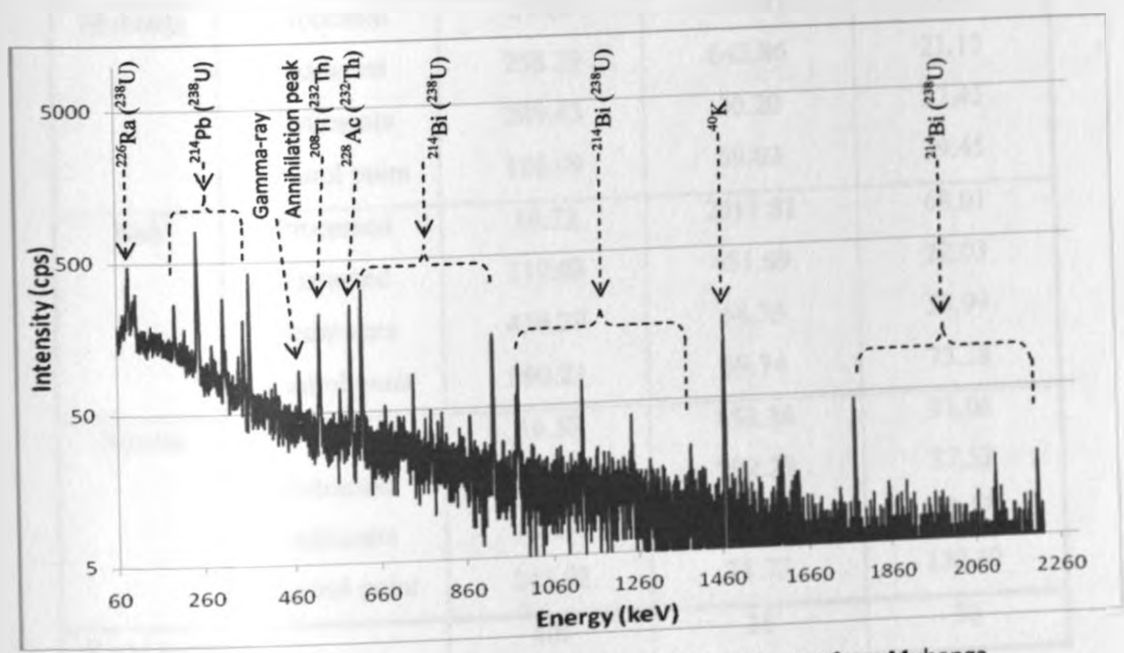
Figure 5.9: Typical gamma-ray spectrum of soil sample from a control point from Muhanga.

61

The result values of radioactivity levels of each natural radionuclide are summarized in Table 5.6. and Figure 5.10. The radioactivity concentrations of ^{40}K, ^{238}U, and ^{232}Th for processed coltan had the ranges 16.58-25.06 Bq kg^{-1} (average: 19.45 Bq kg^{-1}), 853.36-2011.81 Bq kg^{-1} (average: 1279.35 Bq kg^{-1}), and 67.43-91.06 Bq kg^{-1} (average: 75.5 Bq kg^{-1}) respectively.

The range in activity concentrations for extracted coltan are 258.29-334.76 Bq kg^{-1} for ^{40}K (average: 304.1 Bq kg^{-1}), 481.69-792.29 Bq kg^{-1} for ^{238}U (average: 638.9 Bq kg^{-1}) and 21.5-37.53 Bq kg^{-1} (average: 26.9 Bq kg^{-1}) for ^{232}Th.

Table 5.6: Average activity concentration (Bq kg^{-1}) of radionuclides.

Site	Ore Type	^{40}K (Bq kg^{-1})	^{238}U (Bq kg^{-1})	^{232}Th(Bq kg^{-1})
Muhanga	Processed	25.06	972.89	67.43
	Extracted	258.29	642.86	21.15
	Sediments	289.43	50.20	27.45
	Control point	186.99	69.03	39.45
Ruli	Processed	16.72	2011.81	68.01
	Extracted	319.08	481.69	22.03
	Sediments	436.29	64.33	55.99
	Control point	590.21	69.74	73.38
Ngoma	Processed	16.58	853.36	91.06
	Extracted	334.76	792.29	37.53
	sediments	489.41	70.76	49.12
	Control point	245.92	71.33	132.49
World average		400	35	30
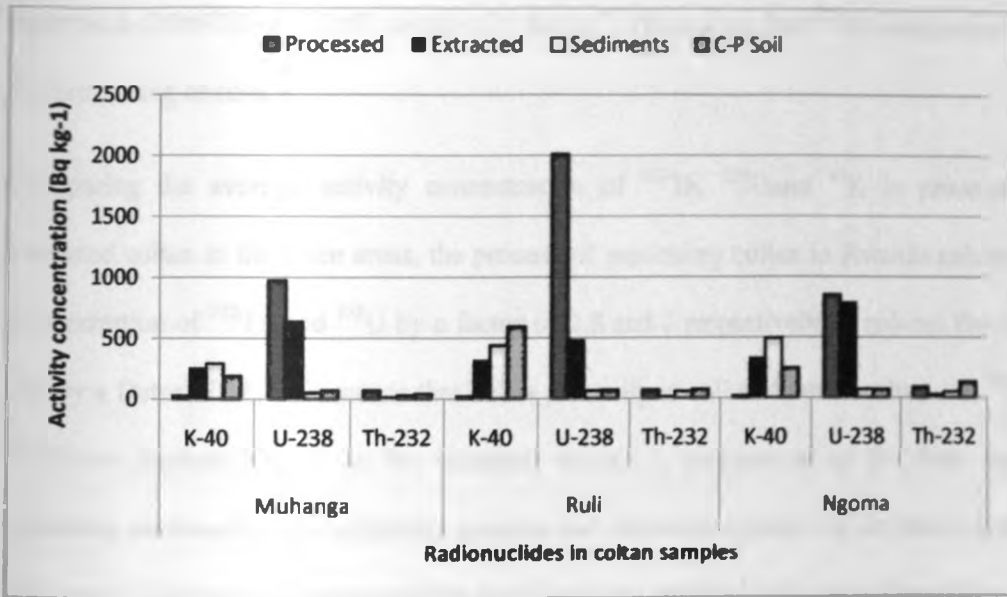
Figure 5.10: Levels of K-40, U-238, and Th-232 in samples from Muhanga, Ruli, and Ngoma.

Sediment samples yielded activity concentration in Bq kg^{-1} of 289.43-489.49 (average: 405.04) for ^{40}K, 50.20-70.76 (average: 61.70) for ^{238}U and 27.45-55.99 (average: 44.18) for ^{232}Th.

The average activity concentration of ^{238}U in all samples exceed the world average reported by UNSCEAR (2000) which is 35 Bq kg^{-1}, while the average ^{40}K activity is below the world average of 400 Bq kg^{-1} (UNSCEAR, 2000) for processed coltan. In all the samples from the three regions, the activity concentrations of ^{40}K were below 500 Bq kg^{-1} with the processed being the lowest (< 30 Bq kg^{-1}). This implies that ^{40}K component primary is in the soil samples and not the ore.

The average activity in ^{232}Th for processed coltan and sediments is greater than the word average, while the average ^{232}Th activity for extracted coltan is below the world average

reported by UNSCEAR (2000) which is 30 Bq kg^{-1}. This means that ^{232}Th is enhanced during the processing of coltan.

Comparing the average activity concentration of ^{232}Th, ^{238}Uand ^{40}K in processed and extracted coltan in the three areas, the process of processing coltan in Rwanda enhances the concentration of ^{232}Th and ^{238}U by a factor of 2.8 and 2 respectively. It reduces the level of ^{40}K by a factor of 15. This means that ^{40}K is primarily in soil and not in coltan ore; ^{238}U and ^{232}Th are masked by soil in the extracted coltan. A comparison of the three naturally occurring radionuclides in sediments samples and the control point did not show significant differences thus the sediments could be considered not enriched with the radionuclides.

5.3 Multivariate chemometric analysis of heavy metals and artificial radionuclides

Multivariate analysis was performed using Unscrambler, version 9.5 software. Pattern recognition methods including Principal Component Analysis (PCA) and Hierarchical Cluster Analysis (HCA) were applied to the data sets. Before running the multivariate algorithm, each variable (each column of the data matrix) was mean centered in order to adjust the data set.

5.3.1 Principal Component Analysis (PCA)

PCA allows the transformation and visualization of complex data sets into a new perspective in which the most relevant information is made more obvious in reduced dimensions. It also probes the structures in the analytical data. PCA was used in this study to identify heavy elements which are more relevant for determining the quality and location of Rwandan coltan. In PCA the data matrix is decomposed into score and loading matrices. The scores

vectors, also called the map of samples, describe the relationship between the samples in the PCA model and the loadings vectors describe the importance of each descriptor or variable within a PCA model. PCA results were validated by using the cross-validation method.

i) Classification of coltan according to their types using PCA.

The PCA results for classifying samples according to coltan types using heavy metals and radionuclides are illustrated in score plots (Figure 5.11 and Figure 5.13) and loading plots (Figure 5.12) respectively.
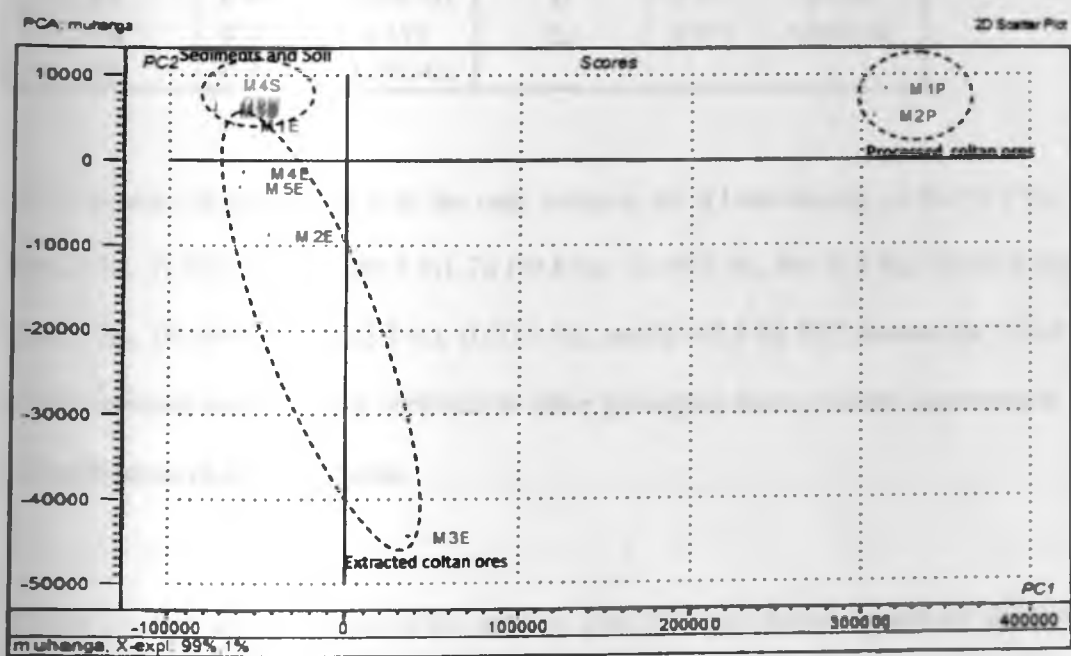

Figure 5.11: PCA score plot of various samples over Muhanga.

M1P and M2P stand for processed coltan from 2 different sampling sites from Muhanga
M1E-M5E stands for extracted coltan from 5 different sampling sites in Muhanga
M1S-M5S stands for sediments from 5 different sampling sites from Muhanga

65

Figure 5.11 shows the score plot of various samples from Muhanga. We note two principle components PC1 and PC2 which may be attributed to variation in the elemental concentrations that are associated with the coltan mineral.

Table 5.7: First two principal components for data from Muhanga.

ELEMENT	PC1	PC2	ELEMENT	PC1	PC2
Sn	0.977	0.214	Br	0.374	0.176
Ca	0.953	0.117	Rb	-0.306	0.235
Ti	0.958	0.229	Sr	0.837	0.119
Mn	0.995	-8.41E-02	Th	0.999	-9.08E-03
Zn	0.998	5.88E-02	Y	0.827	0.14
Ta	0.998	-5.80E-02	U	0.721	0.101
Pb	0.708	0.119	Zr	0.953	4.86E-02
Nb	0.999	-3.39E-02			

PC1 explains in general 99 % of the total variance, but it loads heavily on Sn (97.7 %), Ca (95.3 %), Ti (95.8 %), Mn (99.5 %), Zn (99.8 %), Ta (99.8 %), Pb (70.8 %), Nb (99.9 %), Sr (83.7 %), Th (99.9 %), Y (82.7 %), U (72.1 %), and Zr (95.3 %). PC2 account for 1% of the total variance and it may be attributed to other geological factor of least importance in the classification of coltan minerals.

There are four distinct groups in the samples from Muhanga namely processed ores (green color), sediments (red color), extracted ores (dark blue) and soil (light blue). The relations among the heavy metals based on variation in the ores i.e processed ore (high concentration) and sediments (low concentration) are negatively correlated as indicated in Figure 5.11. Likewise a negative correlation between sediments and extracted ores can be explained by variation in their respective elemental concentration. Both sediments and soil correlate positively. This means that after processing (i.e after removing coltan dependent elements)

sediments have the same heavy element concentration as control point soil. Sample ME3 seems to be an outlier because it separated from the rest.

The relations among the heavy metals (variables) based on the first two principal components are illustrated in Figure 5.12 in two dimensions.
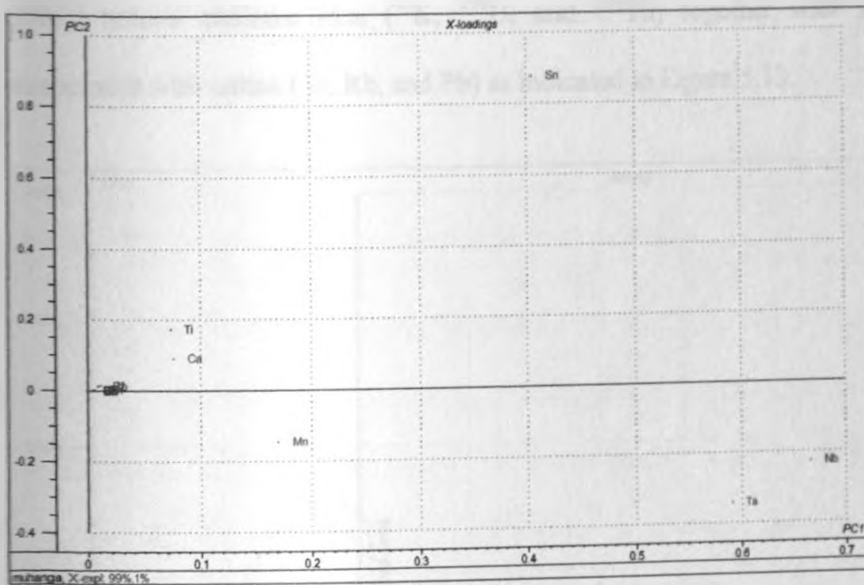
Figure 5.12: PCA correlation loadings plot over Muhanga.

Figure 5.12 reveals that coltan dependent elements i.e Ta, Sn and Nb are located with the highest positive loadings in PC1. Score plot (Fig 5.12) also shows that processed coltan samples (MP1, MP2) are located at positive scores of PC1 and well separated from the rest. Thus, processed coltan samples have strong concentration of Ta, Nb and Sn with lower concentration of the rest of heavy metals.

Ti and Ca are featured with positive loadings in PC2. Score plot (Figure 5.12) also shows that sediments and soil (i.e M1S, M2S, M3S, M4S, M5S and CPM) are located at positive score of PC2. This implies that sediments and soil have highest concentration of Ti and Ca.

67

The PC1 loadings profile show positive value of Zn, Ga, As, Pb, Br, Rb, Sr, Th, Y, U, and Zr while PC1 scores indicate negative values of extracted coltan samples (M1E, M2E, M3E and M4E). This means that extracted coltan samples have lower concentrations of Zn, Ga, As, Pb, Br, Rb, Sr, Th, Y, U, and Zr. M3E seems to be an outlier since it is situated far from the rest.

Similar observations were made on both the score and correlation plots over Muhanga by using natural radionuclides (^{40}K, ^{238}U, and ^{232}Th) together with radioactive elements associated with coltan (Sr, Rb, and Pb) as indicated in Figure 5.13.
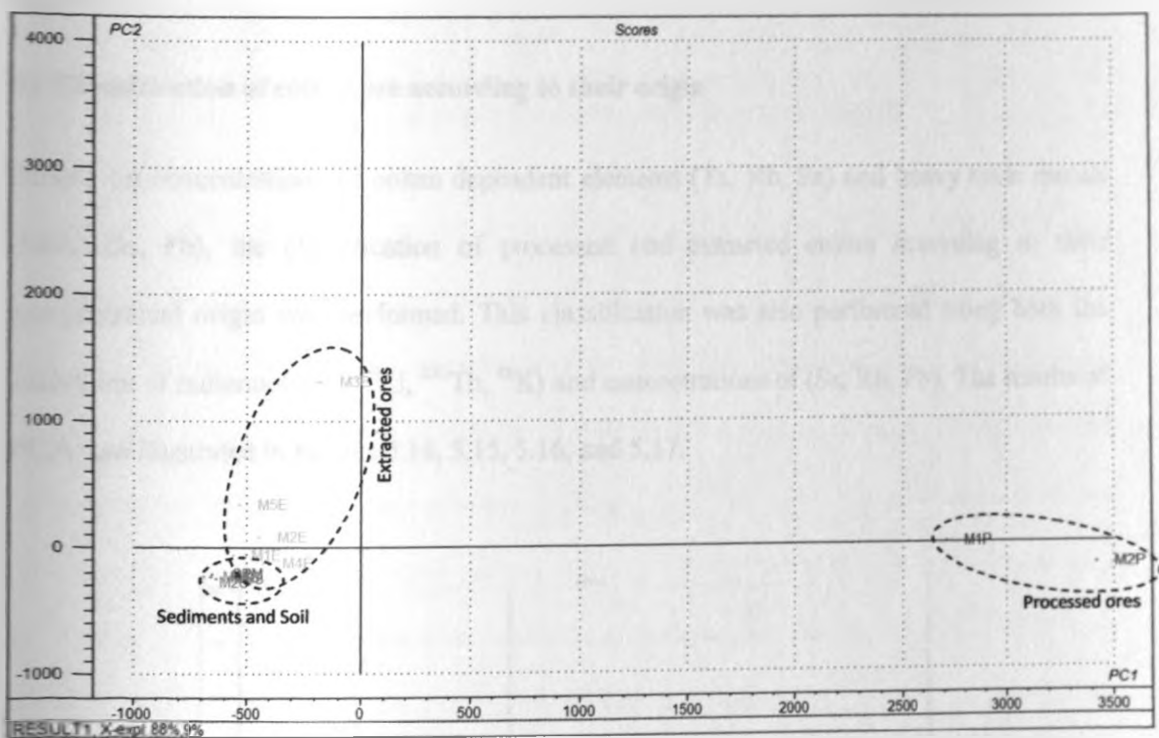
Figure 5.13: Score plot of various samples by using radionuclides (Muhanga).

Similar to the results shown for heavy metals (Figure 5.11), Figure 5.13 indicated 3 patterns in the coltan samples over Muhanga. These patterns may be related to the coltan type. The first group is composed of processed ores (M1P and M2P) in blue color; the second group is characterized by extracted ores (M1E, M2E, M3E, M4E, and M5E) in light blue color; and

68

the third group combines sediments and soil in red color (M1S, M2S, M3S, M4S, and M5S) and soil from control point (CPM) in green color. PCA was not able to separate sediments and soil from the control point. This is because after processing the coltan ore, the remaining sediments have the same chemical characteristics as the local soil drawn from a background location not associated with the coltan underlying rock.

Principal component analysis of heavy metals and radionuclides variables over Ruli and Ngoma reveal similar patterns as indicated in appendixes (A1, A2, A3, A4).

ii) Classification of coltan ore according to their origin

Based on concentrations of coltan dependent elements (Ta, Nb, Sn) and heavy toxic metals (Mn, Zn, Pb), the classification of processed and extracted coltan according to their geographical origin was performed. This classification was also performed using both the activities of radionuclides (^{238}U, ^{232}Th, ^{40}K) and concentrations of (Sr, Rb, Pb). The results of PCA are illustrated in figures 5.14, 5.15, 5.16, and 5.17.

Figure 5.14: PCA score plot for processed coltan using radionuclides
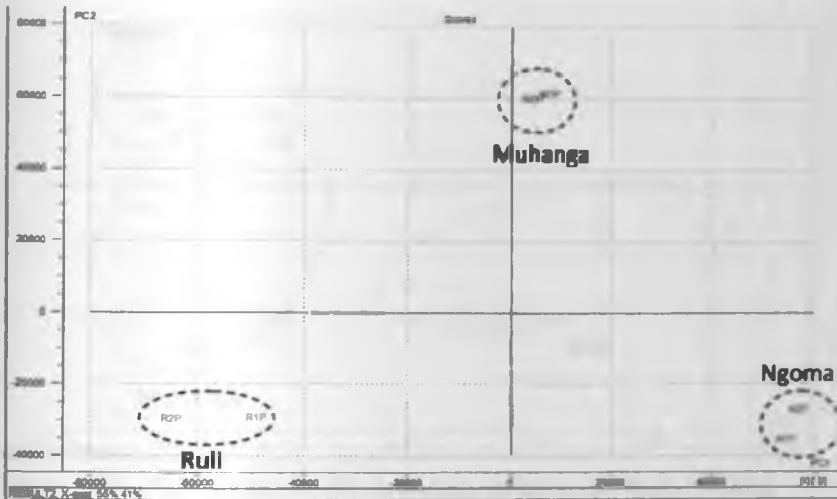
Figure 5.15: PCA score plot of processed coltan samples using coltan dependent elements and heavy toxic metals.

PCA applied to processed coltan samples using radionuclides (^{238}U, ^{232}Th, ^{40}K) and concentration of Sr, Rb, Pb to processed coltan samples shows that there are 3 separate groups (Figure 5.14). This was also observed for coltan dependent elements (Ta, Nb, Sn) and heavy toxic elements (Mn, Zn, Pb) (Figure 5.15). Radionuclides concentration was high and accounted for 91% on PC1 as indicated in Figure 5.14. Heavy toxic metals concentrations seems to be lower in the processed samples which accounts for about 55% on PC1 as shown in Figure 5.15. This shows that concentrations of radionuclides are significant in indicating the origin of coltan as compared to that of heavy toxic elements. PCA was also applied to extracted coltan samples as illustrated in figures 5.16 and 5.17.
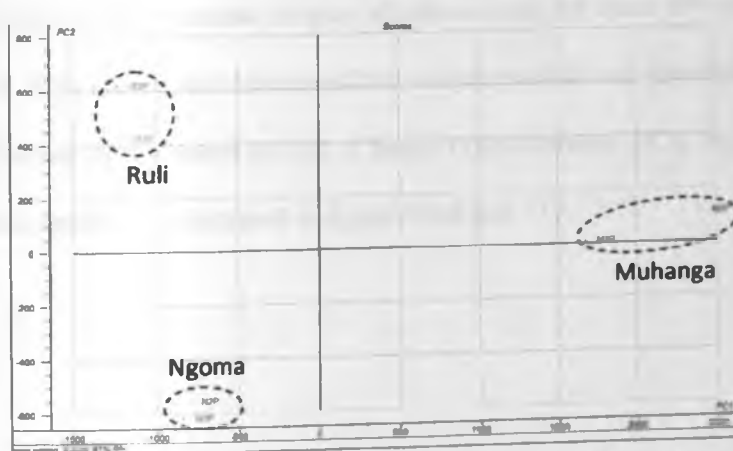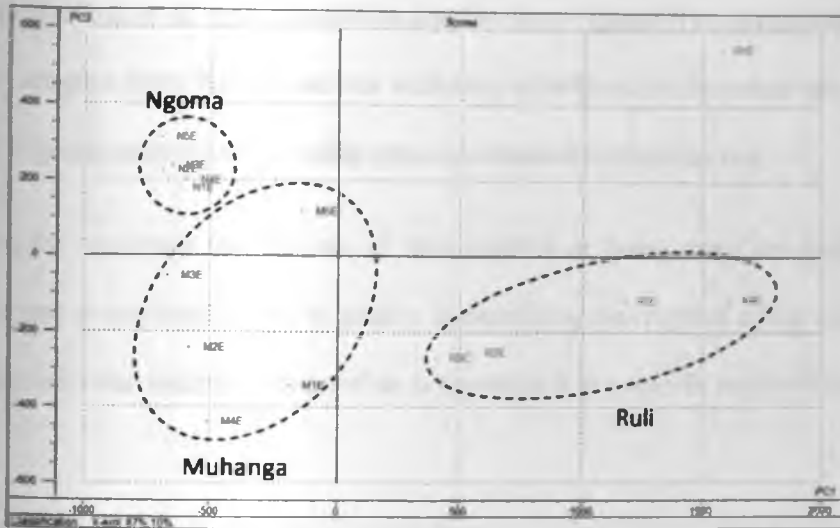
Figure 5.16: PCA score plot for extracted coltan using radionuclides
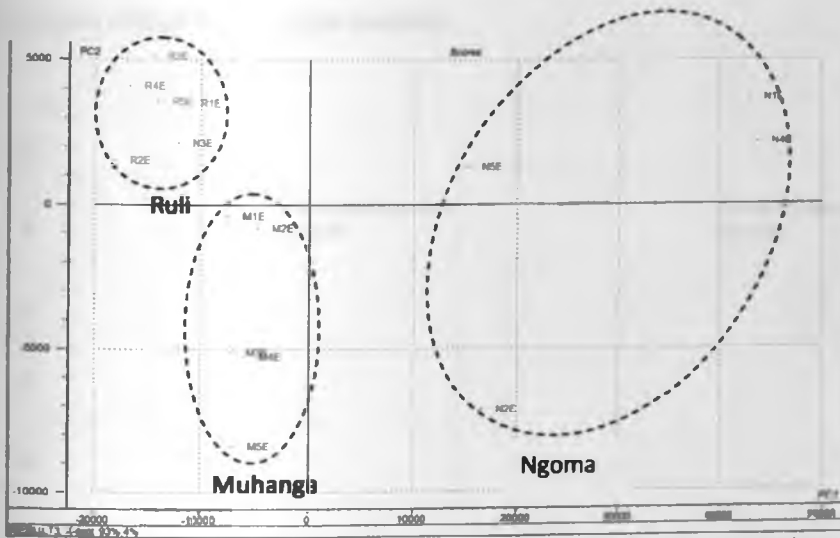
Figure 5.17: PCA score plot for extracted coltan using coltan dependent
elements (Ta, Nb, Sn) and heavy toxic elements (Sn, Pb, Mn)

As noted earlier on processed coltan, PCA reveals three groups the extracted coltan as
observed in Figure 5.16 and Figure 5.17. The explained variance for PC1 using radionuclides
was 87 % while that of heavy metals was 97 %. This shows that heavy metals as well as
radionuclides can be used to classify extracted coltan according their origin. Figure 5.17
shows that samples from Ngoma are scattered indicating that there is a significant variation in

the concentration of heavy metals in samples from Ngoma. This reveals that radionuclides from samples from Ngoma are not uniformly distributed in the coltan ore. Sample (N3E) from Ngoma seems to be an outlier since it is situated far from the rest.

It can be concluded that the use of radionuclides or heavy metal irrespective of whether processed or extracted coltan is suitable in classifying the origin of coltan mineral i.e given a sample of coltan mineral, it is possible to apportion it to a specific region of origin.

5.3.2 Hierarchical Cluster Analysis (HCA)

Hierarchical cluster analysis was used in this study to determine the relationships among heavy metals related to columbite-tantalite.
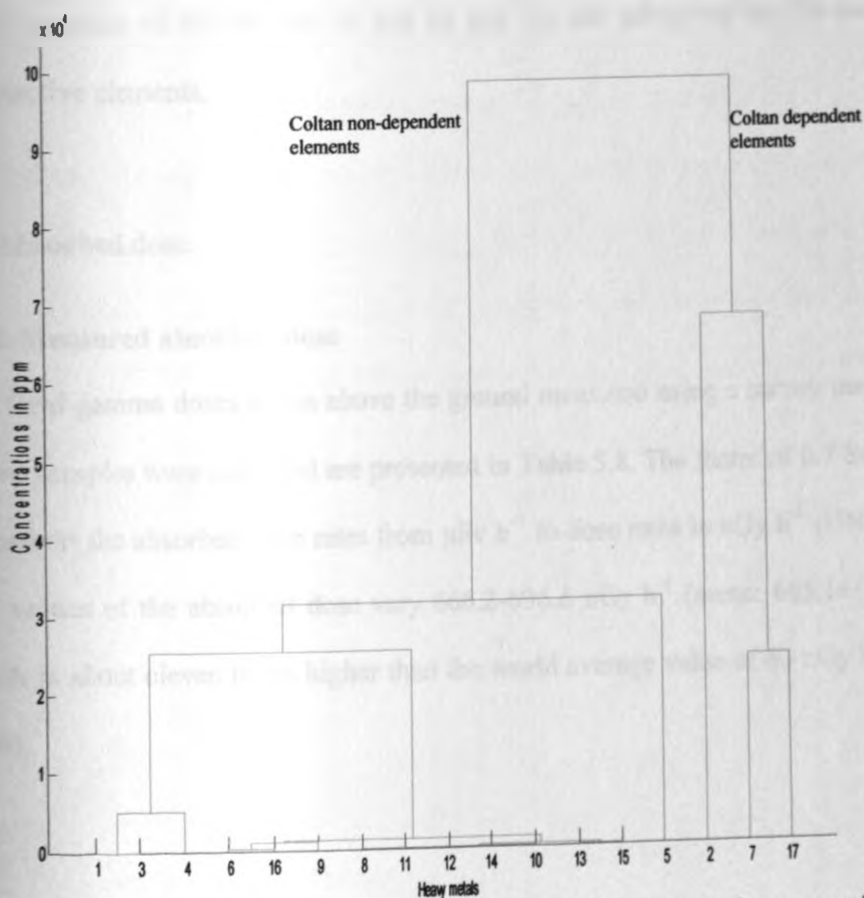
Figure 5.18: Hierarchical Cluster analysis of heavy metals from Muhanga samples.

Figure 5.18 shows that elemental results of heavy metals from Muhanga can be classified into two main groups or clusters. The first cluster is characterized by indices 2, 7 and 17 corresponding to Sn, Ta and Nb respectively. This cluster is also subdivided into 2 sub clusters. The first sub-cluster is characterized by indices 7 and 17 corresponding to Ta and Nb respectively and the second sub-cluster is characterized by Sn. Ta and Nb are normally associated more strongly with coltan and may be used to characterize the quality of columbite-tantalite. Thus it is not surprising that Ta and Nb form the same sub-cluster.

The second group is characterized by indices 1, 3, 4, 5, 6, 8, 9, 10, 12, 13, 14, 15, and 16 corresponding to K, Ca, Ti, Mn, Zn, As, Pb, Br, Rb, Sr, Th, Y, U, and Zr respectively. This group is subdivided into four sub-groups. The first sub-group has K, Ca and Ti elements, the second sub-group consisting of Zn, Zr and Pb which are heavy toxic elements, the third sub-group consists of As, Rb, Sr, Y, and Br and the last sub-group has Th and U which are radioactive elements.

5.4 Absorbed dose

5.4.1 Measured absorbed dose

The field gamma doses at 1m above the ground measured using a survey meter in each area where samples were collected are presented in Table 5.8. The factor of 0.7 Sv Gy^{-1} was used to convert the absorbed dose rates from $\mu Sv\ h^{-1}$ to dose rates in nGy h^{-1} (UNSCEAR, 2000). The values of the absorbed dose vary 666.2-696.6 nGy h^{-1} (mean: 685.1±104.17 nGy h^{-1}), which is about eleven times higher than the world average value of 60 nGy h^{-1} (UNSCEAR, 2000).

Table 5.8: Measured absorbed doses.

Muhanga	Abs. dose (nGy h^{-1})	Ruli	Abs. dose (nGy h^{-1})	Ngoma	Abs. dose (nGy h^{-1})
Site 1	518.34	Site 1	522.35	Site 1	730.39
Site 2	650.80	Site 2	680.25	Site 2	563.81
Site 3	729.43	Site 3	726.45	Site 3	657.78
Site 4	796.92	Site 4	733.31	Site 4	664.49
Site 5	610.79	Site 5	820.68	Site 5	845.71
Average	666.26	Average	696.61	Average	692.44
CPM	650.55	CPR	507.43	CPN	552.06
Global Av.	55	Global Av.	55	Global Av.	55

CP = Control point, M = Muhanga, R = Ruli, N = Ngoma

5.4.2 Calculated absorbed dose

The absorbed dose rates in air due to terrestrial gamma ray at 1m above the ground were calculated from ^{238}U, ^{232}Th and ^{40}K activity concentration values in coltan, sediments and soil assuming that the other radionuclides, such as ^{137}Cs, ^{90}Sr and uranium ^{235}U decay series can be neglected as they contribute very little to the total dose from environmental background (Kocher and Sjoreen, 1985). The conversion factors used to calculate the absorbed dose rates are given in equation 4.2. The average calculated absorbed doses vary 249.15-402.66 nGy h^{-1} (mean: 324.12 nGy h^{-1}). Table 5.9 summarizes the values of the calculated absorbed dose rates in air.

Table 5.9: Calculated absorbed dose in nGy h^{-1}.

Muhanga	Abs. dose (nGy h^{-1})	Ruli	Abs. dose (nGy h^{-1})	Ngoma	Abs. dose (nGy h^{-1})
Site 1	147.14	Site 1	507.16	Site 1	415.64
Site 2	207.01	Site 2	160.32	Site 2	436.47
Site 3	779.07	Site 3	211.04	Site3	429.07
Site 4	114.30	Site 4	200.03	Site 4	424.45
Site 5	355.22	Site 5	167.22	Site 5	307.69
Average	320.55	Average	249.15	Average	402.66
CPM	63.52	CPR	101.15	CPN	123.23
Global Av.	55	Global Av.	55	Global Av.	55

These results show that the average absorbed in air is 6 times the world average value reported by UNSCEAR (2000) and comparable with the other high background radiation areas in the world as illustrated in Table 5.10. This characterizes Rwanda mining areas as a High Background Radiation Areas (HBRA).

Table 5.10: Comparison of absorbed dose rates in Rwanda with other areas of the world.

Country	Absorbed dose	References
Orisa, India	1925 (nGy h^{-1})	Mohanty et al., 2004
Lambwe, Kenya	949.31 (nGy h^{-1})	Achola, 2009
Minas, Brazil	220 (nGy h^{-1})	Malanca et al., 1993
Minjingu, Tanzania	1415 (nGy h^{-1})	Banzi et al., 1999
Firtina valley, Turkey	77.4 (nGy h^{-1})	Kurnaz et al., 2007
Zonguldak, Turkey	71.1 (nGy h^{-1})	Emirhan and Ozben, 2009
Xiazhuang granite, China	124 (nGy h^{-1})	Yang et al., 2005
Eskisehir, Turkey	167 (nGy h^{-1})	Orgun et al., 2005
Eastern Desert, Egypt	488 (nGy h^{-1})	Arafa, 2004
Rwanda	324.12 (nGy h^{-1})	Present study

Measured absorbed dose rates in air are far much higher than the calculated absorbed dose rates. This may be attributed to the fact that measured absorbed dose includes dose from cosmic rays. Another reason for the difference is that measured absorbed dose includes contribution due to radon while calculated does not include radon.
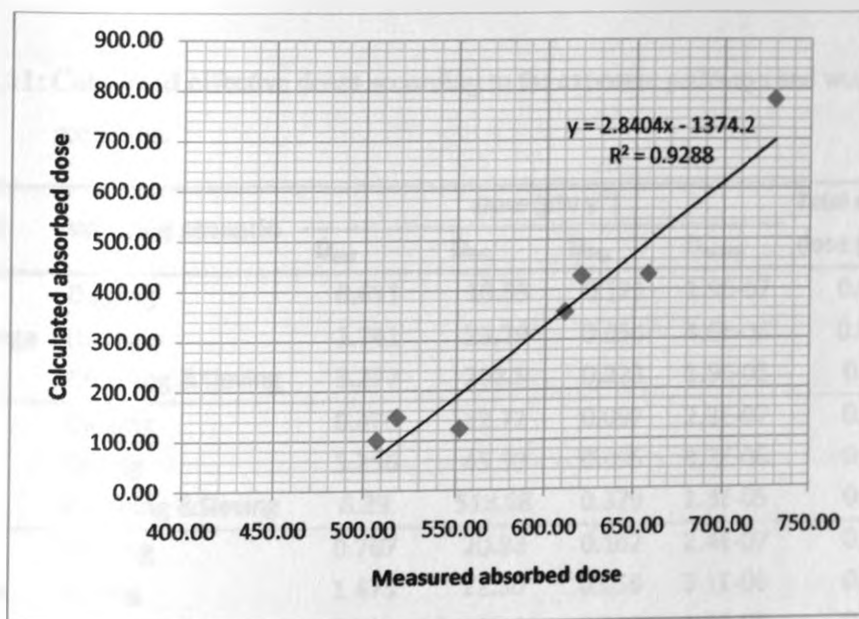
Figure 5.19: Correlation of calculated absorbed dose and measured absorbed dose.

5.5 Results of effective dose

The dose calculated according to the exposure pathways and working scenarios is given in Table 5.11. D_{ext} is the external dose due to gamma-rays emitted by radionuclides contained in the environment; D_{inh} is the internal dose due to the inhalation of air contaminated with dust from the ore. D_{ing} is the internal dose due to inadvertent ingestion of radionuclides and D_{subm} is the external dose due to submersion in contaminated air. The total effective dose is the sum of all the contributions. The values of the total effective doses vary 0.0173-0.272 mSv y^{-1} in Muhanga, 0.013-0.525 mSvy^{-1} in Ruli and 0.022-0.255 mSv y^{-1} in Ngoma. The most significant pathway (98 %) is the inhalation of Coltan bearing dust and the least

significant is the external exposure from submersion in contaminated air. A study conducted by Mustapha et *al.* (2007) on the occupational radiation exposures of the artisans mining columbite-tantalite in the Eastern Democratic Republic of Congo which neighbours Rwanda shows similar observations. Similar results were also observed by Odumo, (2009) in a gold mining in Southern Nyanza of Kenya.

Table 5.11: Calculated effective doses according to the exposure pathways and working scenarios.

AREAS	Working scenario	Dose (μSv y^{-1})				Total effective dose (mSv y^{-1})
		D_{ext}	D_{inh}	D_{ing}	D_{subm}	
Muhanga	Digging	0.611	16.55	0.121	1.9E-07	0.0173
	Drying	1.741	23.79	0.056	4.6E-06	0.0256
	Crushing &Sieving	3.277	268.5	0.223	1.9E-05	0.271
Ruli	Digging	0.476	12.72	0.097	2.3E-07	0.013
	Drying	3.256	45.99	0.095	3.2E-06	0.049
	Crushing &Sieving	6.29	518.98	0.379	1.3E-05	0.525
Ngoma	Digging	0.767	20.98	0.162	2.4E-07	0.022
	Drying	1.475	22.30	0.058	3.1E-06	0.024
	Crushing &Sieving	2.799	251.6	0.233	1.2E-05	0.254

The result presented in Table 5.11 shows that all the values of the total effective dose are below 1 mSv y^{-1} and 20 mSv y^{-1} which are the values recommended by ICRP for the public and occupational exposure respectively. However, care must be taken since it is believed that radiation at any level poses a health risk. To reduce risk due to inhalation of coltan dust, respiratory protection for contamination such as dust-mask should be provided to artisan workers; local ventilation equipment should be used to exhaust the dust away from coltan mills. The miners should also avoid mixing home utensils with the equipments used in the mines in order to decrease possible exposure pathways. Access of the members of the public to the mines and mine tailings should be minimized to prevent the members of the public from dispersing them or using them for building, etc

Chapter 6

6.0 CONCLUSION AND SUGGESTIONS FOR FURTHER WORK

6.1 Conclusion

The concentration of heavy metals in coltan ores, sediments and soil has been studied in this work using Energy Dispersive X-Ray Fluorescence (EDXRF) spectrometry. Heavy elements detected included three groups: Heavy elements which are normally associated with coltan (Tantalum (Ta), Niobium (Nb), Tin (Sn)), radioactive elements associated with coltan (Uranium (U), Thorium (Th), and Potassium (K)) and heavy toxic metals (Lead (Pb), Zinc (Zn), Manganese (Mn)). Elements associated with coltan (Ta (30.6 %), Nb (25.7%) and Sn (16.4 %)) were abundant especially in processed coltan and extracted coltan. Some sediments samples show also a little concentration of Ta (< 0.008 %) and Nb (<0.006 %). The lower presence of Nb and Ta in the sediments confirms the improved methods used by the artisanal miners in the extraction of coltan. However, for full economic realization better processing technologies need to be considered. Toxic elements such as Pb, Zn and Mn were noted in all samples with Mn having the highest concentration. Radioactive elements (U, Th & K) were also measured. Processed coltan and extracted coltan indicated the highest concentration. In most sediments samples the level of U, Th and K were below the detection limit.

Activity concentration of primordial radionuclides, ^{40}K, ^{238}U and ^{232}Th series in samples of samples of coltan, sediments and soil were generated in this study. The average activity concentration of ^{40}K, ^{238}U and ^{232}Th in coltan ore, sediments and soil are 267.4, 521.5 and 57.1 Bq kg^{-1} respectively. The average activity concentration of ^{238}U in all samples was 15 times higher than the world average activity concentration. In all processed coltan the average

activity concentration of ^{40}K was below the global average activity concentration reported by UNSCEAR (2000). The activity concentration of ^{232}Th in processed coltan and sediments was higher than the world average activity concentration recommended by UNSCEAR. In extracted coltan the activity of ^{232}Th was below the word average activity concentration.

Absorbed dose was obtained by both model of calculation and measurements. The measured dose rate (685.1 nGy h^{-1}) was far higher than the calculated dose rate (324.12 nGy h^{-1}). This could be attributed to the fact that calculated absorbed dose does not include cosmic rays. Another reason for the difference is that, measured absorbed dose may not have come from the sampled (coltan ore) rock only; it could have originated from somewhere else due wind dispersion of radioactive aerosol. Based on the high level of measured and calculated dose compared to the world average dose (55 nGy h^{-1}), coltan mining areas of Rwanda was characterized as a High Background Radiation Areas (HBRA).

The annual effective dose from each working scenario (i.e digging, drying, crushing and severing) were also determined by model of calculation. The results of effective dose calculation showed that the most significant pathway of exposure (0.35 mSv y^{-1}) is inhalation of coltan bearing dust while crushing and sieving coltan.

Chemometric techniques viz; Principal Component Analysis (PCA) and Hierarchical Cluster Analysis (HCA) were used to clasify coltan samples according to ore type (Processed coltan, Extracted coltan, Sediments and Soil) and the origin of the sample (Muhanga, Ruli and Ngoma).

6.2 Suggestions for further work

Based on the results and conclusions drawn from this study the following suggestions for further work are recommended:

1) Follow-up studies should investigate the human risk effect associated with the mining of coltan, the impact of the mining activities on the public living near these mining areas and the impact of mining activities on the environment.

2) Further studies should be done on the measurement of radon level in mine washing water and on health implications in relation to high radiation doses.

3) Further assessment of radiation exposure due to NORM should be carried out in the whole country and consider not only coltan but also other minerals of economic importance.

REFERENCES

Achola, S.O., 2009, Radioactivity and elemental analysis of carbonatite rocks from parts of Gwasi area, south western Kenya, M.Sc. Thesis, University of Nairobi, Unpublished.

Aly, A.A., Hassan, M.H. and Huwait, M.R.A., 1999, Radioactivity assessment of fabricated phosphogypsum mixtures, Fourth Radiation Physics Conference, 15–19 November 1999, Alexandria, Egypt, pp. 632–640.

Arafa, W., 2004, Specific activity and hazards of granite samples collected from the Eastern Desert of Egypt, J. Environ. Radioact. 75, pp. 315-327.

Banzi, F.P., Leonard, D.K. and Felician, M.B., 1999, Natural radioactivity and radiation exposure at the Minjingu phosphate mine in Tanzania, J. Radiol. Prot. 20, p. 41-51

Bennett, B.G., 1997, Exposure to natural radiation exposure worldwide. In: Processings of the Fourth International Conference on High Levels of Natural Radiation: Radiation Doses and Health Effects, Beijing, China, 1996. Elsevier, Tokyo, pp. 15-23.

Brouwer, P., 2003, Theory of XRF, PANalytical BV, The Netherlands.

CIA (Central Intelligence Agency), 2000, Rwanda: World Factbook 2000, U.S., p. 415-417.

Chougaonkar M.P., Eappen K.P., Ramachandran T.V., Shetty P.G., Mayya, Y.S., Sadasivan, S. and Venkat V. R., 2003, Profiles of doses to the population living in the high background radiation areas in Kerala, India, Health, Safety and Environment Group, Bhabha Atomic Research Centre, Mumbai 400 085, India.

Crouthanel, C.C., 1975, Applied Gamma Spectroscopy, Pergmon Press, Newyork.

Delco B., 1996, Dose rate conversion factors, soil thickness and their influence on natural background dose rate in air above carbonate terrains, J. Environ. Radioactivity 31, pp. 51-70.

Dixon, D.W., Gooding, T.D. and McCready-Shea, S., 1996, Evaluation and significance of radon exposures in British workplace buildings, Environ. Int. 22, pp. 1079–S1082.

EC (European Commission), 2002, Practical use of the concepts of clearance and exemption and exemption, Part II, application of the concepts of exemption and clearance of natural radiation sources, Radiation Protection vol 122. Part II (Luxembourg: EC).

Eggermont, G., 1990, Recommendations of the Belgium Council on Science Policy, paper presented at the first International Seminar on managing indoor radon problem, MOI, Belgium 14th May 1990.

Eckerman, K.F. and Rayman J.C., 1993, Federal Guidance Report N0 12, External exposure to radionuclides in air, water and soil (Washington, DC: US Environmental Protection Agency Office of Radiation and Indoor Air) EPA.

Emirhan, M.E. and Ozben, C.S., 2009, Assessment of radiological risk factors in the Zonguldak coal mines, Turkey, J. Radiol. Prot. 29 (2009) 527-534

Fuat, Y., 2000, NBTA: a program for columbite-group minerals in rare-element granites and granitic pegmatites, Computer & Geosciences 27 (2001) 241-248.

Funtua, I.I. and Elegba, S.B., 2005, Radiation exposure from high-level radiation area and related mining and processing activities of Jos Plateau, central Nigeria, International Congress Series 1276: pp. 401– 402.

Ghiassi-nejad, M., Mortazavi, S.M.J., Cameron, J.R., Niroomand-rad, A. and Karam, P. A., 2002, Very High Background Radiation Areas of Ramsar, Iran: Preliminary Biological Studies, Health Physics 82, Number 1

Gooding, T.D. and Dixon, D.W., 1992, Radon in UK workplaces, Radiat. Prot. Dosimetry 45: pp. 187–189.

Gordon R.G., 2008-2nd Edition, Practical Gamma-Ray Spectrometry, Warrington, UK.

Gupta, C.K. and Suri A.K., 1994, Extractive Metallurgy of Niobium, CRC Press, USA.

Hedwig, D. and Maenhaut, W., 1990, Application of principal component and cluster analysis to the study of the distribution of minor and trace elements in normal human brain, Chemometrics and Intelligent Laboratory Systems, 9, 273-286.

IAEA (International Atomic Energy Agency), 2005, Quantitative X-ray Analysis System, Documentation version 2.0, Seibersdorf, Austria.

IAEA (International Atomic Energy Agency), 2004, Application of the Concepts of Exclusion, Exemption and Clearance, Safety Series No. RS-G-1.7 (Vienna: IAEA).

IAEA (International Atomic Energy Agency), 1991, Nuclear Analysis Software Part 2: Gamma Spectrum Analysis, Activity Calculations and Neutron Activation Analysis (GANAAS), Computer manual series No.3 (Vienna, 1991).

Ibrahiem, N.M., Abdel-Ghani, A.H., Shawky, S.M., Ashraf, E.M. and Farouk, M.A., 1993, Measurement of radioactivity levels in soil in the Nile Delta and Middle Egypt. Health Phys. 64: pp. 620–627.

ICRP (International Commission on Radiological Protection), 1994, Protection Against Radon-222 at Home and at Work, ICRP Publication 65, Pergamon Press, Oxford.

ICRP (International Commission on Radiation Protection), 2000, Protection of the public in situations of prolonged radiation exposure ICRP Publication 82; Ann. ICRP 29 (1–2), Pergamon Press, Oxford.

Jasim, U.A., 1990, Radon overview in natural environment and dwellings IAEA, Austria page 269

Karen, H. and Richard, B., 2003, Coltan Mining in the Democratic Republic of Congo: How tantalum-using industries can commit to the reconstruction of the DRC, Fauna & Flora international, Cambridge, UK.

Knoll, G.F., 1997, Radiation Detection and Measurements, John Willey and sons, New York.

Kocher, D.C. and Sjoreen A.L., 1985, Dose-rate conversion factors for external for external exposure to photon emitters in soil, Health Phys 48, pp 193-205.

Kurnaz, A., Küçükömeroğlu, R., Keser, R., Okumusoglu, N.T., Korkmaz, F., Karahan, G. and Çevik, U., 2007, Determination of radioactivity levels and hazards of soil and sediment samples in Firtina Valley (Turkey), Applied Radiation and Isotopes 65 (2007), pp 1281-1289.

Lipsztein, J.L., Dias da Cunha, K.M., Azeredo, A.M.G., Julião, L., Santos, M., Melo, D.R. and Simões, F.F.L., 2001, Exposure of workers in mineral processing industry in Brazil, J. of Environmental Radioactivity 54, pp.189-199.

Malance, A., Gaidolfi, L., Pessina, V. and Dallara, G., 1996, Distribution of ^{226}Ra, ^{232}Th, and ^{40}K in soils of Rio Grande do Norte, Brazil, J. Environ. Radioactiv. 30, pp. 55–67.

Malanka, A., Pessina, V. and Dallara, G., 1993, Assessment of the natural radioactivity in the Brazilian state of Rio Grande, Health hysics 65 (3), pp. 298-302.

Mangala, J.M., 1987, A multi-channel X-ray fluorescence analysis of fluorspar ore and rock from Mrima hill, Kenya, MSc Thesis, University of Nairobi, Unpublished.

Martin, J.E., 2006, Physics for radiation protection (Second Edition), WILEY-VCH Verlag GmbH &Co. KGaA

Massart, D.L., Vandeginste, B.G.M., Buyden, L.M.C., S. de Jong, Lewi P.J. and Smeyers-Verbeke, J., 1998, Handbook of Chemometrics and Qualimetrics, Elsevier Science, Amsterdam, Holland.

Mbuzukongira, P., 2006, Assessment of occupational radiation exposure of artisan miners of columbite-tantalite (coltan) in the Eastern Democratic Republic of Congo, M.Sc. Thesis, University of Nairobi, Unpublished.

McCall, G.J.H., 1958, Geology of the Gwasi area, Ministry of commerce and Industry, Geology survey of Kenya, Dept. No. 45.

Michael F. A., 2003, Handbook of Radioactivity Analysis, Academic Press, Amsterdam.

Mohanty, A.K., Sengupta, D., Das, S.K., Vijayan, V. and Saha, S.K., 2004, Natural radioactivity in the new discovered high background radiation area on the eastern coast of Orissa, India, Radiation measurements 38, 153-165.

Mustapha, A.O., Mbuzukongira, P. and Mangala, M.J., 2007, Occupational radiation exposures of artisans mining columbite-tantalite in the eastern Democratic Republic of Congo, J. Radiol. Prot. 27: pp. 187-195.

Mustapha, A.O., Patel, J.P. and Rathore, I.V.S., 1999, Assessment of human exposures to natural sources of radiation in Kenya, Radiation Protection Dosimetry, Vol. 82, No. 4, pp. 285-292.

NCRP (National Council on Radiation Protection), 1993, Radiation protection in the mineral extraction industry, NCRP Report No.118, Bethesda, MD.

NCRP (National Council on Radiation Protection), 1988, Ionizing Radiation Exposure of the Population of the United States, NCRP Report no. 93, Bethesda, MD.

NCRP (National Council on Radiation Protection and Measurements), 1987, Exposure of the population of the United States and Canada from natural background radiation, Report no. 94, Bethesda, MD.

Nriagu, J.O., 1998, A silent epidemic of environmental metal poisoning? Environ. Pollut. 50, pp 139-161.

Oatway, W.B. and Mobbs, S.F., 2003, Methodology for estimating the doses to member of the public from the future use of land previously contaminated with radioactivity, NRPB-W36 Report, National Radiation Protection Board, Chilton.

Odumo, B.O., 2009, Radiological survey and elemental analysis in the gold mining belt, southern Nyanza, Kenya, MSc Thesis, University of Nairobi, Unpublished.

Orgun, Y., Altinsony, N., Gultekin, A.H., Karahan, G. and Celebi, N., 2005, Natural radioactivity levels in granitic plutons and groundwaters in Southeast part of Eskisehir, Turkey, Appl. Radiat. Isot. 63, pp. 267-275.

Patel, J.P., 1991, Environmental radiation survey of the area of high natural radioactivity of Mrima hill of Kenya, Discovery and Innovation 3(3), pp. 31-36.

Richard G.B., 2007, Applied chemometrics for scientists, University of Bristol, UK, John Wiley & Sons, Ltd.

Risica, S., 2001, Italian basic safety standards legislation, J. Radiol. Prot. 21, 8.

Roskill Information Services. Ltd., 2002, The Economics of Tantalum, 8th Edition, London

Sam, A.K. and Elmahadi M.M., 2008, Assessment of absorbed dose rate in air over Plowed Arable lands in Sinnar State, Central Sudan, Radiation Protection Dosimetry 129(4): p. 473-477.

Scivyer, C.R. and Gregory, T.J., 1995, BRE (Building Research Establishment) Radon in the workplaces

Selvasekarapandian S., Muguntha N.M., Sivakumar R., Balasubramanian S., Venkatesan T., Meenakshisundaram V., Ragunath V.M. and GajendranV., 1999, Gamma radiation dose from radionuclides in soil samples of Udagamandalam (Ooty) in India, Radiation protection dosimetry 82, pp. 225-228.

Sparks, C.J., 1979, Rapid quantitative X-ray fluorescence using fundamental parameters method, Advances in X-ray analysis, Plenum Press, New York.

SSI (Swedish Radiation Protection Institute), 1999, Radon legislation and national guidelines, Åkerblom, G., ISSN: 0282-4434.

Tahir, S.N.A., Jamil, K., Arif, M., Ahmed, N. and Ahmad, S.A., 2005, Measurement of Activity Concentrations of Naturally occurring Radionuclides in Soil Samples from Punjab Province of Pakistan and Assessment of Radiological Hazards, Radiation Protection Dosimetry, 113(4): pp. 421-427.

Taylor and Francis Group, 2006, Practical guide to chemometrics, USA.

Thomas, S., 2008, Geological atlas of Africa: With notes on stratigraphy, tectonics, geohazards and geosites of each country, pp. 189-204.

Tzortzis, M., Svoukis, E. and Tsertos, H., 2004, A comprehensive study of natural gamma radioactivity levels and associated dose rates from surface soils in Cyprus, Radiat. Prot. Dosim. 109: pp. 217–24

UNSCEAR (United Nations Scientific Committee on the Effects of Atomic Radiation), 1993, Sources, Effects and Risk of Ionizing Radiation. Report to the General Assembly, with annexes (New York: UNSCEAR).

UNSCEAR (United Nations Scientific Committee on the Effects of Atomic Radiation), 1998, Sources and effects of ionization radiation, Report to the General Assembly, with Scientific Annexes B: Exposures from Natural Radiation Sources (New York: UNSCEAR).

UNSCEAR (United Nations Scientific Committee on the Effects of Atomic Radiation), 2000, Sources, effects and risks of ionization radiation, Report to The General Assembly, with Scientific Annexes B: Exposures from Natural Radiation Sources (New York: UNSCEAR).

UNSCEAR (United Nations Scientific Committee on the Effects of Atomic Radiation), 2008, Sources and Effects of Ionizing Radiation, Report of the United Nations Scientific Committee on the Effects of Atomic Radiation, Fifty-sixth session, New York, USA.

USEPA (United States Environmental Protection Agency), 2004, A Citizen's Guide to Radon: the Guide to Protecting Yourself and Your Family from Radon, 402-K-02-006.

Varley, N.R. and Flowers, A.G., 1998, Indoor radon prediction from soil gas measurements, Health Phys.74: pp.714–8
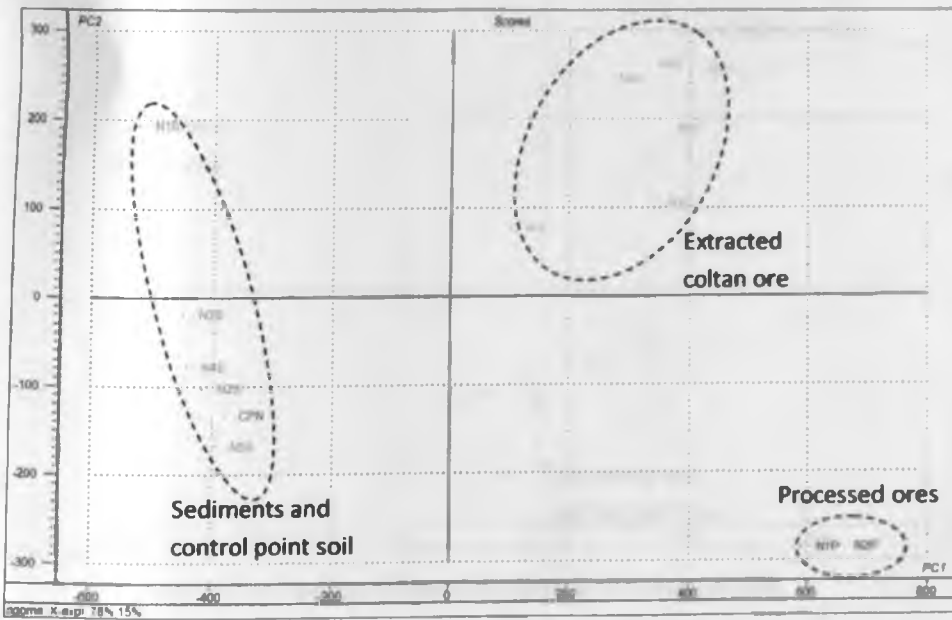
Wei, L., 1980, Health surveys in high background radiation areas in China, Science 209: pp. 877-880.

Yang, Y., Wu, X., Jiang, Z., Wang, W., Lu, J., Lin, J., Wang, L. and Hsia, Y., 2005, Radioactivity concentrations in soils of the Xiazhuang granite area, China Appl. Radiat. Isot. 63, 255-259.
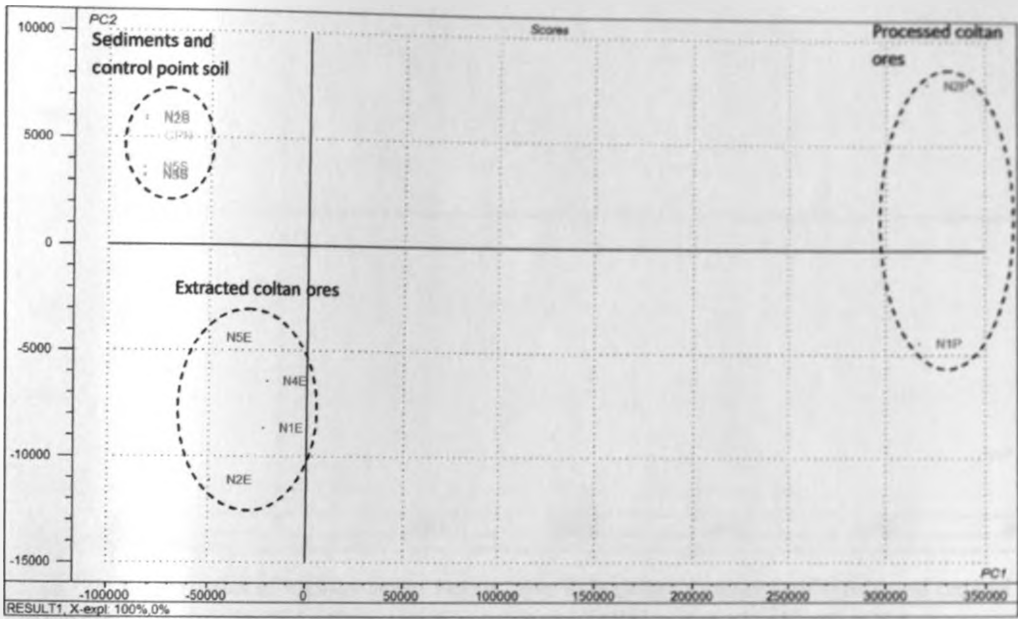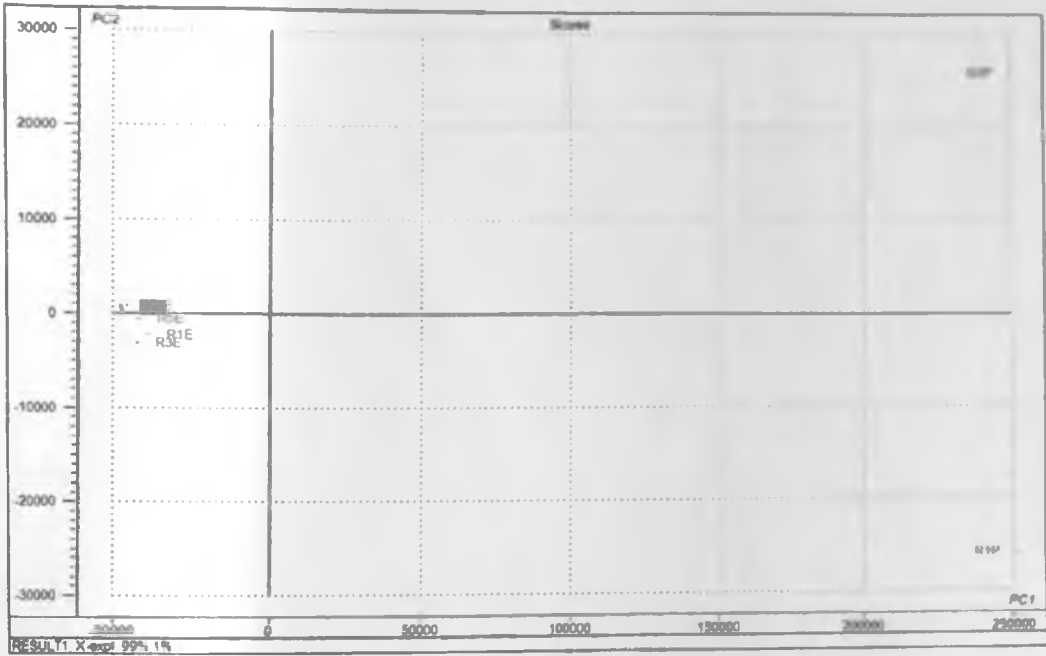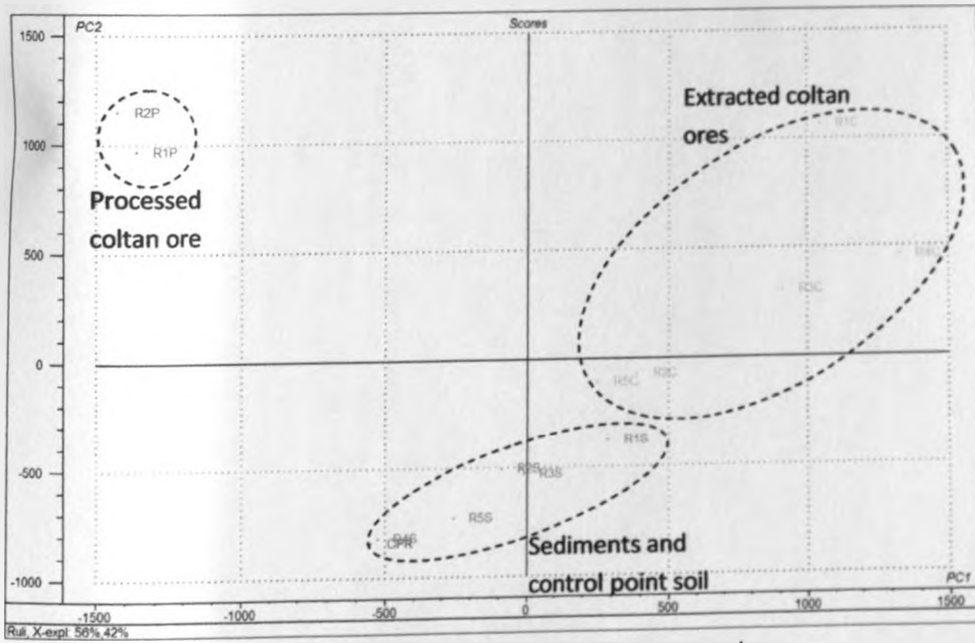
A1: PCA score plot of various heavy metals samples from Ngoma

A2: PCA score plot of various radionuclides of samples from Ngoma

A3: PCA score plot of various heavy metals from Ruli coltan samples (sediments and control point soil: Red color, extracted coltan ore: Blue color, processed coltan ores: Green color.

A4: PCA score plot of various radionuclides from Ruli coltan samples